Larson, P. B., 1976, The metamorphosed alteration zone associated with the Bruce Precambrian volcanogenic massive sulfide deposit, Yavapai County, Arizona: Tucson, University of Arizona, unpublished M. S. thesis, 99 p.

Larson, P. B., 1984, Geochemistry of the alteration pipe at the Bruce Cu-Zn volcanogenic massive sulfide deposit, Arizona: Economic Geology, v. 79, no. 8, p. 1880-1896.

Lavery, N. G., 1985, The use of fluorine as a pathfinder for volcanic-hosted massive sulfide ore deposits: Journal of Geochemical Exploration, no. 23, p. 35-60.

Lawrence, J. R., and Dixon, R. L., 1986, Geology of the Spud Mountain Tuff in the vicinity of the Iron King mine, *in* Beatty, B., and Wilkinson, P. A. K., eds., Frontiers of geology and ore deposits of Arizona and the Southwest: Tucson, Arizona Geological Society Digest 16, p. 370-373.

Lindberg, P. A., 1983, Development of the Verde graben, north central Arizona [abs.]: Flagstaff, Arizona, Arizona-Nevada Academy of Science, 27th Annual Meeting.

Lindberg, P. A., 1986a, An overview of Precambrian ore deposits of southwestern United States, *in* Beatty, B., and Wilkinson, P. A. K., eds., Frontiers of geology and ore deposits of Arizona and the Southwest: Tucson, Arizona Geological Society Digest 16, p. 18-23.

Lindberg, P. A., 1986b, Geology of the Copper Chief mine, Jerome district, Arizona, *in* Beatty, B., and Wilkinson, P. A. K., eds., Frontiers in geology and ore deposits of Arizona and the Southwest: Tucson, Arizona Geological Society Digest 16, p. 343-349.

Lindberg, P. A., 1986c, A brief geologic history and field guide to the Jerome district, Arizona, *in* Nations, J. D., Conway, C. H., and Swann, G. A., eds., Geology of central and northern Arizona: Flagstaff, Arizona, Field trip guidebook for Geological Society of America Rocky Mountain Section Meeting, p. 127-139.

Lindberg, P. A., and Jacobson, H. S., 1974, Economic geology and field guide of the Jerome District, Arizona, *in* Geology of Northern Arizona, Part II, Area studies and field guides: Flagstaff, Arizona, Geological Society of America Rocky Mountain Section Meeting, p. 794-804.

Lindgren, W., 1926, Ore deposits of the Jerome and Bradshaw Mountain quadrangles, Arizona: U. S. Geological Survey Bulletin 782, 192 p.

London, D., and Burt, D. M., 1978, Lithium pegmatites of the White Picacho district, Maricopa and Yavapai Counties, Arizona, *in* Burt, D. M., and Pewe, T. L., eds., Guidebook to the geology of central Arizona: Tucson, State of Arizona Bureau of Geology and Mineral Technology, Special Paper no. 2, p. 60-72.

Lundin, R. L., 1985, The Zonia mine area: Prescott, Arizona, Field guide for Central Arizona Geological Society, 8 p.

McKee, E. H., and Anderson, C. A., 1971, Age and chemistry of Tertiary volcanic rocks in north-central Arizona and their relationship to the Colorado Plateaus: Geological Society of America Bulletin, v. 82, p. 2767-2782.

Meyer, C., 1972, Private company reports and mapping, Jerome, Arizona.

Nutt, C. J., 1984, Strata-bound uranium deposits in the Dripping Spring Quartzite, Gila County, Arizona, U.S.A., *in* Ferguson, J., ed., Proterozoic unconformity and stratabound uranium deposits: Report of the working group on uranium geology organized by the International Atomic Energy Agency TECDOC-315, p. 95-113.

O'Hara, P. F., 1986a, Previous geologic work in the Prescott-Mayer area, Arizona, *in* Beatty, B., and Wilkinson, P. A. K., eds., Frontiers of geology and ore deposits of Arizona and the Southwest: Tucson, Arizona Geological Society Digest 16, p. 355-357.

O'Hara, P. F., 1986b, Stratigraphy and structural geology in the Prescott-Mayer area, Arizona, *in* Beatty, B., and Wilkinson, P. A. K., eds., Frontiers of geology and ore deposits of Arizona and the Southwest: Tucson, Arizona Geological Society Digest 16, p. 358-364.

Otton, J. K., Light, T. D., Shride, A. F., Bergquist, J. R., Wrucke, C. T., Theobald, P. K., Duval, J. S., and Wilson, D. M., 1981, Mineral resources of the Sierra Ancha Wilderness and Salome Study Area, Gila County, Arizona: Summary report, U. S. Geological Survey Miscellaneous Field Investigations Map MF-1162-H, 6 p.

Ransome, F. L., 1933, General geology and summary of ore deposits, *in* Ore deposits of the Southwest: Washington, D. C., 16th International Geologic Congress Guidebook 14, Excursion C-1, p. 1-23.

Sangster, D. F., 1972, Precambrian volcanogenic massive sulfide deposits in Canada; a review: Geological Survey of Canada, Paper 72-22, 44 p.

Shride, A. F., 1967, Younger Precambrian geology in southern Arizona: U. S. Geological Survey Professional Paper 566, 89 p.

Slatt, R. M., Heintz, G. M., Lowry, P. H., and O'Hara, P. F., 1978, Precambrian Pike's Peak iron-formation, central Arizona, *in* Burt, D. M., and Pewe, T. L., eds., Guidebook to the geology of central Arizona: Tucson, State of Arizona Bureau of Geology and Mineral Technology, Special Paper No. 2, p. 73-82.

Stan West Mining Corporation, 1983, Annual Report: Phoenix, Arizona, 18 p.

Stensrud, H. L., and More, S., 1980, Precambrian geology and massive sulfide environments of the west-central Hualapai Mountains, Mohave County—A preliminary report, *in* Jenney, J. P., and Stone, C., eds., Studies in western Arizona: Tucson, Arizona Geological Society Digest 12, p. 155-165.

Still, A. R., 1974, Review of geology and recommendations for exploration, Antler mine and adjacent areas, Mohave County, Arizona: Tucson, private report prepared for Standard Metals Corp., 32 p.

Swan, M. M., Hausen, D. M., and Newell, R. A., 1982, Lithological, structural, chemical, and mineralogical patterns in a Precambrian stratiform gold occurrence, Yavapai County, Arizona, *in* Hausen, D. M., and Parks, W. C., eds., Process metallurgy: New York, American Institute of Mining, Metallurgical, and Petroleum Engineers, p. 143-157.

Welty, J. W., Reynolds, S. J., Keith, S. B., Gest, D. E., Trapp, R. A., and DeWitt, E., 1985, Mine index for metallic mineral districts of Arizona: Tucson, Arizona Bureau of Geology and Mineral Technology Bulletin 196, 92 p.

White, D., 1986, Gold distribution at the United Verde Extension, a massive base-metal sulfide deposit, Jerome, Arizona, *in* Beatty, B., and Wilkinson, P. A. K., eds., Frontiers in geology and ore deposits of Arizona and the Southwest: Tucson, Arizona Geological Society Digest 16, p. 330-338.

Wrucke, C. T., Otton, J. K., and Desborough, G. A., 1986, Summary and origin of the mineral commodities in the Middle Proterozoic Apache Group in central Arizona, *in* Beatty, B., and Wilkinson, P. A. K., eds., Frontiers in geology and ore deposits of Arizona and the Southwest: Tucson, Arizona Geological Society Digest 16, p. 12-17.

Revised manuscript accepted 1987.

in Jenney, J. P., and Reynolds, S. J., 1989, Geologic evolution of Arizona: Tucson, Arizona Geological Society Digest 17, p. 211-238.

PROTEROZOIC ANOROGENIC GRANITES OF THE SOUTHWESTERN UNITED STATES

by
J. Lawford Anderson

Department of Geological Sciences
University of Southern California
Los Angeles, California 90089

ABSTRACT

The mountain ranges of Arizona and adjacent California and Nevada contain large areas underlain by Proterozoic anorogenic granites comprising the southwesternmost portion of the 1.4- to 1.5-Ga-old transcontinental belt. Of these, a biotite ± muscovite, monazite-bearing suite resides in central and southeastern Arizona as part of a peraluminous segment that extends through New Mexico into the Colorado Front Range. This group is bordered on the south (southern Arizona to Sonora) and west (Colorado River region) by a marginally peraluminous to metaluminous granitic suite bearing biotite-sphene ± hornblende, fluorite.

All of these 1.4-Ga-aged granites are distinctly more potassic, iron-enriched (relative to Mg), and depleted in Ca, Mg, and Sr in contrast to most older orogenic granitoids that make up much of the host terrane. In general, the large-ion lithophile-element enriched character of these granites is a consequence of limited melting of a water-deficient crustal source at depths greater than 25 to 37 km. For the peraluminous anorogenic suite, this contrast is less extreme, perhaps resulting from a larger degree of melting as a consequence of a greater metasedimentary component and water in its crustal source.

The anorogenic granitic magmas intruded into the upper crust at depths of 8 to 17 km or shallower at temperatures up to 790°C. The most dramatic variation in the crystallization-intensive parameters resides in the oxygen fugacity, which spans three orders of magnitude. Relative to other anorogenic suites, all of the magmas crystallized at elevated levels of fO_2, as reflected in their assignment to the anorogenic magnetite series. Yet a regionally significant rise in primary fO_2 levels, unmatched elsewhere in the transcontinental belt, occurs for plutons in western Arizona, including the Holy Moses and Hualapai granites. The most extreme case is the Hualapai granite whose biotite Fe-Fe + Mg ratios drop, due to high fO_2, to a low of 0.27 down from more typical levels of 0.54 to 0.75. Such extreme variations in primary levels of oxygen fugacity must be an indirect imprint of regional changes of the level of oxidation of the lower crust. This area of western Arizona is in proximity to the eastern limit of the 1.4-Ga biotite ± hornblende granites, a boundary that is also approximately equivalent to major changes in the Nd isotopic composition of these granites and the metamorphic and magmatic character of the older orogenic terranes.

On a global scale, the crust-forming orogenies ended by 1.6 Ga and the continents entered a long-lived era dominated by localized extension and transcontinental intrusion of anorogenic potassic rapakivi granite, mafic dike swarms, charnockite, and anorthosite. Perhaps plate consumption became intraoceanic during this time. The profuse and widespread nature of the igneous activity has no Phanerozoic analogue and is considered to be unique to the Proterozoic. A crustal overturn model ties the magmatism to heating within a largely undepleted subcontinental mantle, the eventual rise of mantle plumes, and the transfer of heat into the youthful, undifferentiated Proterozoic crust. Subsequent melting and rise of potassic granitic magmas from the lower crust leads to considerable crustal reorganization, a process that would continue until both the mantle and crust reached a stable configuration.

INTRODUCTION

After 300 million years of orogenesis, the Proterozoic North American craton entered a new era of tectonic quiescence beginning about 1.6 Ga ago. This preceding period of deformation and igneous activity was a time of principal continental growth by episodic crust formation represented by south- to southwestward-younging orogenic terranes, which range in age from 1.82 to 1.90 Ga (Penokean orogeny) and 1.61 to 1.68 Ga (Mazatzal orogeny). The oldest members of these orogenic belts are almost always supracrustal metasedimentary and mafic to felsic metavolcanic rocks intruded by variably foliated granitoid masses, which usually have a calc-alkaline composition. For the next 600 million years, this newly formed Proterozoic crust, unlike the older Archean, continued to undergo considerable modification involving deep-seated crustal melting, leading to widespread anorogenic intrusion of epizonal, potassium-rich granites into the upper crust. For many areas, the presence of associated mafic intrusions, including large volumes of older gabbro to anorthosite and swarms of diabase, indicates that this thermal disturbance was probably rooted in the mantle. To date, three principal periods of anorogenic igneous activity have been defined: (1) 1.41 to 1.49 Ga, (2) 1.34 to 1.40 Ga, and (3) 1.0 to 1.2 Ga. By far, the first was most profound and constitutes over 60 complexes forming a transcontinental belt (fig. 1) over 1,000 km wide, extending from Labrador to southern California (see J. L. Anderson, 1983, for a more comprehensive review and appropriate references).

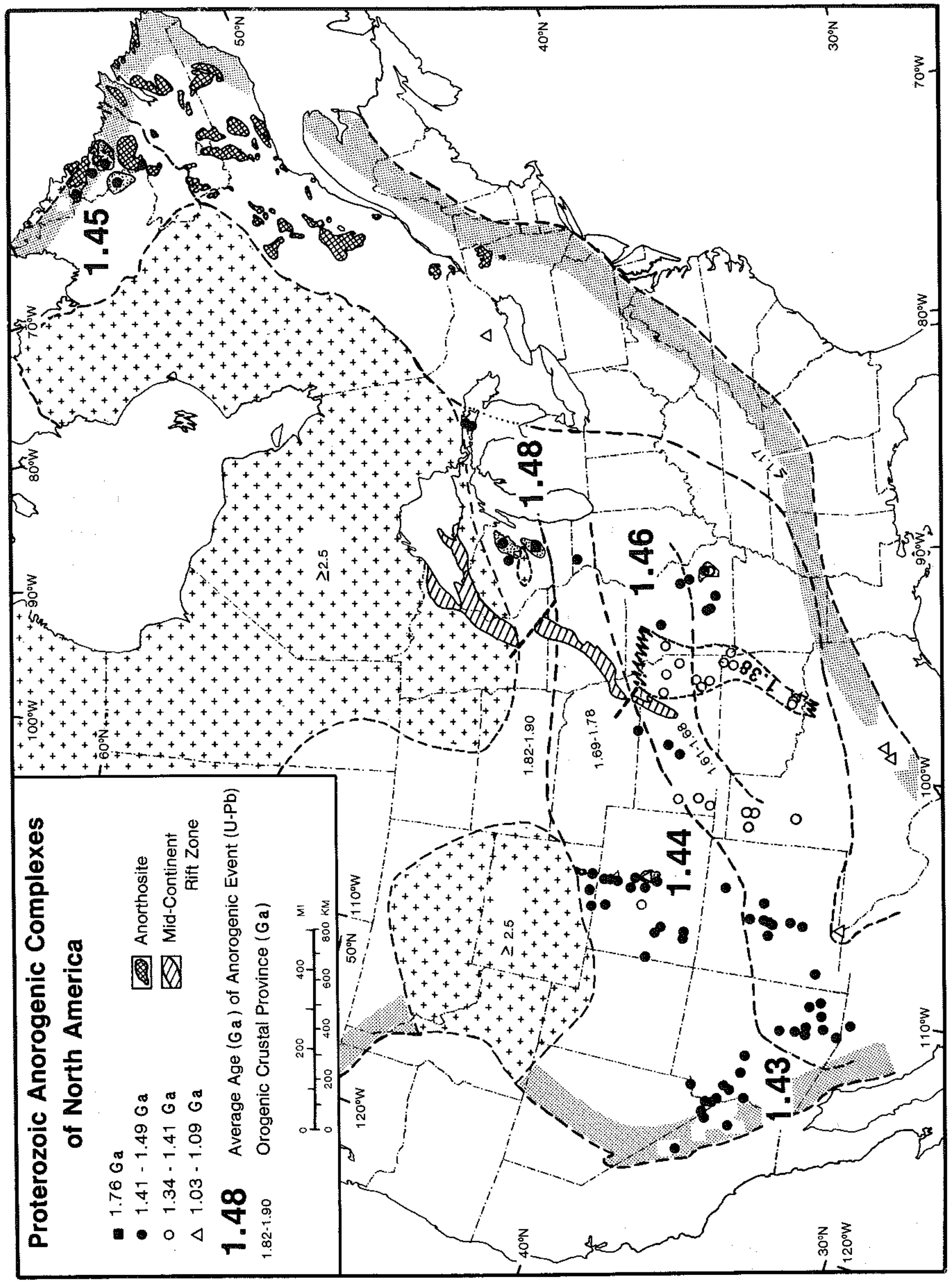

Figure 1. Distribution of Proterozoic anorogenic granite complexes of North America. Modified from Anderson (1983).

The Precambrian terranes of Arizona and adjacent Nevada and California contain vast areas underlain by nonfoliated granitic batholiths. Although some of these represent late kinematic orogenic intrusions (ca. 1.65 Ga), most are part of the anorogenic transcontinental belt. Silver (1968) was the first to recognize their existence in the southwestern United States and their regional context. Twenty-two separate intrusions are listed in table 1 and depicted on a regional map in figure 2. From their unique textural characteristics, however, many others have been inferred to exist, but have been insufficiently studied to merit inclusion at this time.

A principal attribute of these granites is the K-feldspar megacrystic or porphyritic nature. Previous workers, including Volborth (1962, 1973), Silver and others (1981), and Kwok (1983) have acknowledged the affinity of these rocks to rapakivi granites. This assignment is appropriate. Although well-developed rapakivi texture has been noted only for portions of the Gold Butte granite, the original usage of this term by Finnish geologists refers not to a texture but a suite of anorogenic granites that possess a number of attributes, including: (1) an epizonal nature of intrusion (discordant, postkinematic plutons that are often circular in outline), (2) a preponderance of K-feldspar relative to plagioclase, (3) low water content (expressed in the form of late hydrous silicate crystallization and lack of pegmatites), and (4) enrichment in fluorine, certain large-ion lithophile elements (LILE), including K, Rb, Ba, REE, Th, Nb, and U, and Fe relative to Mg. As described by Vorma (1971), rapakivi texture is only well developed in the wiborgite variety of rapakivi. Other textural types include pyterlitic (seriate with ovoidal K-feldspar), even-grained, and porphyritic. Although all of these textural types are represented in the southwestern United States, the porphyritic variety (fig. 3) is by far the most common.

Rapakivi in Finnish means "rottenstone." In his original description of the Ruin granite, Ransome (1903, p. 74) noted that the rock is "generally decomposed" forming "gentle slopes . . . often covered with what might be termed granite crumbs—a coarse angular sand consisting of quartz crystals, and fragments of pinkish feldspar, and flakes of biotite." Similarly disintegrated outcrops of the 1.49-Ga Wolf River batholith of Wisconsin have long been mined as a sand and gravel resource. On U. S. Geological Survey topographic maps, these sites are appropriately designated as "rottenstone quarries."

The intrusions composing the transcontinental belt range over 80 Ma in age. The older complexes occur in the midcontinent with ages of about 1.49 Ga. Systematic younging occurs to the southwest (see references in J. L. Anderson, 1983). In this region, all appear younger than 1.44 Ga with some of the youngest ages (1.40 to 1.41 Ga, J. Wright, 1984, personal commun.) occurring in western Arizona and adjacent California.

Other than the Parker Dam and Bowmans Wash plutons, none of the granites included in this paper have received a published detailed petrologic study of mineralogical and compositional variations. Yet there is a variety of general geologic to geochronologic information that is helpful (see references in table 1). It is hoped that this review and preliminary analysis will set the stage for further study of this remarkable plutonic episode.

PETROGRAPHIC VARIATIONS

One objective of this work is to seek out any systematic regional variations within this suite of granite intrusions. Specific descriptions and general references are given in table 1. As depicted in figure 4, most range in composition from monzogranite to syenogranite. The exceptions are the Continental granodiorite, the Holy Moses quartz monzonite, and the Bowmans Wash quartz monzodiorite.

Although the K-feldspar is megacrystic in most of these granites, petrographic analysis reveals that this mineral phase poikilitically enclosed and began to crystallize after that of plagioclase and usually quartz in every specimen studied. Toward the K-feldspar rims, other phases also occur as inclusions, including Fe-Ti oxides, apatite, zircon, allanite, and hydrous silicates. In addition, biotite, commonly with muscovite or hornblende, is uniformly late in crystallization, after that of the feldspars, quartz, and most of the accessory phases. Hence, the hydrous silicate minerals are not visibly prominent, but rather anhedral and interstitial to the fundamental mineral framework of the host rock. Such textural features are indicative of the relative dryness of the magma system, a feature also consistent with the paucity of pegmatites and aplites and general lack of hydrothermal contact effects. Exceptions to these generalizations include the Marble, Fort Huachuca, and Oracle granites, which contain euhedral and visibly prominent biotites. Moreover, pegmatites are less rare in the central Arizona granites and are notably common in a few, including the Oracle and Lawler Peak granites.

Accessory phases include fluorapatite, zircon, allanite, and Fe-Ti oxides. The mineralogy of the latter is significant. Ishihara (1977) noted that anorogenic granites commonly comprise an ilmenite series" where magnetite is low in abundance to absent. The transcontinental anorogenic belt is an exception to this generalization. To date, only the 1.49-Ga Wolf River batholith (J. L. Anderson, 1980, 1987) has been shown to be of the ilmenite series. Elsewhere, including the Southwest, the granites belong to an "anorogenic magnetite series," a feature attributable to crystallization under an elevated level of oxygen fugacity. This important aspect is developed further in later sections of this paper.

Despite these general textural and mineralogic attributes, significant variations exist in the hydrous-phase mineralogy from which follow other differences in accessory mineralogy and general chemical compositional features. A large number of these granites are moderately peraluminous and contain biotite, often with muscovite, and occasionally garnet (fig. 2). All reside in central to southeastern Arizona,

TABLE 1. Proterozoic Anorogenic Plutons of the Southwestern U.S.

No.	Pluton	Description	Age[1](Ga)	$^{87}Sr/^{86}Sr^{1}$	General[2] Reference
1	Gold Butte granite, Nevada	Coarse-grained porphyritic to seriate biotite ± hornblende monzogranite. Intrudes high-grade terrane of granulite gneisses, foliated charnockites, and minor anorthosite. Rapakivi mantling of feldspar locally well developed but not widespread. Accessory phases includes sphene, magnetite, allanite, apatite, zircon, and occasionally fluorite. Plagioclase An_{22-26}. Color index: 9 to 12.	1.425±.025 (U/Pb) [1]		12-15
2	Beer Bottle Pass granite, Lucy Grey Range, Nevada	Coarse-grained porphyritic hornblende biotite syenogranite. Partial rapakivi mantles common. Weak to moderate foliation becomes protomylonitic at contact with older gneissic granite. Accessory phases include sphene, Fe-Ti oxides, apatite, allanite, and zircon. Color index: 18 to 20.	1.425±.025 (U/Pb) [1]		33
3	Newberry granite, Newberry Mts., Nevada	Dark-colored, coarse-grained, porphyritic to seriate hornblende biotite monzogranite. Ovoidal K-feldspar phenocrysts (20-30%) up to 6 cm long. Weakly to strongly foliated by mid-Mesozoic(?) deformation. Accessory phases include sphene, Fe-Ti oxides (magnetite, ilmenite), allanite, apatite, and zircon. Color index: 14 to 21. Plagioclase An_{33-40}.	1.425±.025 (U/Pb) [1]		14-16
4	Davis Dam granite, Nevada and Arizona	Similar to and possibly equivalent to Newberry granite. More felsic with greater abundance of K-feldspar phenocrysts. No hornblende. Color index: 11 to 17. Plagioclase: An_{24-27}.	1.425±.025 (U/Pb) [1]		14-16
5	Dead Mountains granite, Dead Mtn., Nevada and California	Equigranular coarse-grained biotite syenogranite. Leucocratic, pinkish rock with low color index (1 to 2). Accessory phases include magnetite, sphene, allanite, apatite, and zircon. Plagioclase An_{25-34}.	1.425±.025 (U/Pb) [1]		14-16
6	Homer granite, Homer Mts., California	Coarse-grained seriate biotite monzogranite. Quartz and biotite interstitial to subhedral K-feldspar (to 2 cm) and plagioclase (An_{24-28}). Leucocratic with low color index of 4 to 5. Accessory phases include magnetite, sphene, apatite, and zircon.			14,15
7	Marble granite, Marble Mts., California	Coarse-grained, porphyritic biotite monzogranite to syenogranite. Blocky K-feldspar phenocrysts (2-5 cm, 15-20%). Medium-grained matrix contains idiomorphic quartz and plagioclase (An_{22-40}). Accessory phases include magnetite, sphene, apatite, zircon, and late-magmatic allanite and fluorite. Color index: 3 to 9.	1.43 (U/Pb) [2]		14, 15
8	Holy Moses quartz monzonite, Hualapai Mts., Arizona	Coarse-grained seriate to locally porphyritic biotite hornblende quartz monzonite. Phenocrysts of K-feldspar and plagioclase (An_{22-29}) less than 2 cm in size, set in a fine- to medium-grained matrix. Accessory phases include magnetite, sphene, allanite, apatite, zircon, and rare fluorite. Color index: 4-10.	1.335±.023 (Rb/Sr) [3]	0.7094 [3]	14,15,17
9	Hualapai granite, Hualapai Mts., Arizona	Coarse-grained, seriate (pyterlitic) hornblende biotite syenogranite. Ovoidal to oblong K-feldspar locally crowded. Minor granophyre. Magmatic foliation occurs along contacts. Accessory phases include magnetite, sphene, allanite, apatite, zircon, and fluorite. Plagioclase: An_{16-22}. Color index: 3 to 5.	1.367±.069 (Rb/Sr) [3]	0.7032 [3]	14, 15, 17
10	Bowmans Wash quartz monzonite, Whipple Mts., California, Arizona	Gray-colored, medium-grained hornblende biotite quartz monzodiorite to quartz monzonite and monzogranite. Distinctively spotted with polycrystalline clots of hornblende and late-magmatic biotite. Border phase, finer grained with K-feldspar and plagioclase phenocrysts, occurs as stope blocks in the Parker Dam granite. Accessories include magnetite and lesser amounts of ilmenite (altered to ferropseudobrookite), allanite, apatite, sphene, and zircon. Plagioclase: An_{27-39}. Color index: 22 to 33.	1.407±.004 (U/Pb) [4]		18-21
11	Parker Dam granite, Whipple Mts., California, Arizona	Coarse-grained porphyritic hornblende biotite syenogranite to monzogranite. K-Feldspar phenocrysts are abundant (34 to 70%) and moderately to strongly aligned. Magmatic foliation, intensified to protomylonite at contacts, is enhanced to mid-Mesozoic(?) shear zones. Accessories include magnetite and lesser amounts of ilmenite (altered to ferropseudobrookite), sphene, allanite, apatite, sphene, and zircon. Plagioclase: An_{24-29}. Color index: 2 to 18.	1.401±.005 (U/Pb) [4]	0.7042 [5]	18-21
12	Lawler Peak granite, Bagdad region, Arizona	Crudely zoned circular pluton. Main phase is a porphyritic biotite and two-mica monzogranite that grades into several interior masses of porphyritic muscovite monzogranite. Phenocrysts of K-feldspar oriented into a magmatic flow foliation. Uraniferous with a variety of accessory phases including manganilmenite, magnetite, rutile, zircon, fluorite, allanite, monazite, apatite, xenotime, and thorite. Plagioclase: An_{10-20}. Color index: 2 to 3.	1.411±.003 (U/Pb) [6]		22
13	Dells granite, near Prescott, Arizona	Medium-grained, equigranular two-mica monzogranite. Locally porphyritic. Uraniferous with accessories of magnetite, ilmenite, garnet, tourmaline, fluorite, zircon, and thorite. Plagioclase: An_{10}. Color index: 2 to 3.	1.400±.015 (U/Pb) [6]		23
14	Sierra Estrella granite, Southern Sierra Estrella Mts., Arizona	Medium- to coarse-grained, porphyritic biotite (marginal variant) and two-mica monzogranite. Muscovite subordinate to biotite. Accessory phases include magnetite and less ilmenite, allanite, apatite, zircon, and rare monazite. Plagioclase: An_{34-38}. Color index: 5 to 6.	1.380 (Rb/Sr) [7]	0.7050 [7]	33
15	Ak-Chin granite, Northern Table Top Mts., Arizona	Coarse-grained, seriate, two-mica monzogranite to syenogranite. Leucocratic with biotite predominant over muscovite. Large alkali feldspar poikilitic with inclusions of quartz and plagioclase and, near margins, biotite, magnetite, and apatite. Accessory phases include magnetite and less ilmenite, monazite, allanite, apatite, xenotime, zircon, and rare fluorite. Plagioclase: An_{15-24}. Color index: 4 to 5.			33
16	Ruin granite, Globe District, Arizona	Coarse-grained porphyritic biotite and two-mica monzogranite. Phenocrysts of K-feldspar (to 4 cm long) exhibit local alignment. Accessory phases include magnetite and less ilmenite, monazite, apatite, and zircon. Plagioclase: An_{32-36}. Color index: 8 to 11.	1.440±.020 (U/Pb) [6]	0.7015 [8]	24, 25
17	Oracle granite, northern Santa Catalina Mts., Arizona	Coarse-grained porphyritic biotite and two-mica monzogranite. Euhedral biotite is conspicuous. Intrudes Pinal Schist. Muscovite minor in abundance when present. Occurrence of rare hornblende in Picacho and Tortolita Mtns. (Banks, 1980) is atypical. K-feldspar phenocrysts (to 7 cm) poikilitically enclose matrix phases. Severely mylonitized in portions of Santa Catalina and Tortilita Mts. Accessory phases include magnetite and less ilmenite, monazite, apatite, zircon, and in quartz, rutile. Plagioclase: An_{33-39}. Color index: 5 to 16.	1.440±.020 (U/Pb) [9]	0.7065 [8]	25-28
18	Stockton Pass granite, Pinaleno Mts., Arizona	Medium- to coarse-grained, porphyritic two-mica monzogranite. Biotite occurs disseminated and in distinct polycrystalline clots. Granophyric intergrowths common. Accessory phases include magnetite, sphene, apatite, and zircon.	1.405±.065 (Rb/Sr) [10]	0.7101 [10]	29
19	Granite of Ladybug Saddle, Pinaleno Mts., Arizona	Medium- to coarse-grained, porphyritic two-mica monzogranite. Massive to weakly foliated. Biotite occurs in distinctive, polycrystalline clots. Accessory phases include magnetite, sphene, allanite, apatite, and zircon. Plagioclase: An_{30-34}. Color index: 412.	1.384±.039 (Rb/Sr) [10]	0.7101 [10]	29
20	Tungsten King granite, Little Dragoon Mts., Arizona	Medium- to coarse-grained, porphyritic biotite and two-mica syenogranite. Zoned K-feldspar phenocrysts to 4 cm in length. Accessory phases include magnetite, apatite, zircon, and sphene. Plagioclase: An_{5-10}. Color index: 4 to 5.	1.420 (U/Pb) [11]		29
21	Continental granodiorite Santa Rita Mts., Arizona	Coarse-grained, porphyritic, mafic hornblende biotite to biotite granodiorite and monzongranite. Intrudes Pinal Schist. Mafic xenoliths common. K-feldspar phenocrysts (0-5%) up to 4 cm long. Accessory phases include prominent sphene and less amounts of magnetite, apatite, allanite, and zircon. Plagioclase: An_{27-35}. Color index: 20 to 30.	1.430 (U/Pb) [11]		31
22	Fort Huachuca granite, Huachuca Mts., Arizona	Coarse-grained, porphyritic biotite monzogranite. K-feldspar phenocrysts to 5 cm in length, contain inclusions of plagioclase and quartz. Accessory phases include magnetite and lesser amounts of ilmenite, large wedge-shaped sphene, allanite, apatite, and zircon. Plagioclase: An_{31-44}. Color index 7 to 16.	1.4254±.025 (U/Pb) [11]		32, 33

[1]Age References: [1] Silver, cited by Stewart and Carlson (1978); [2] Silver and McKinney (1962); [3] Kessler (1976); [4] J. L. Anderson and Wright (in prep.); [5] Davis and others (1982); [6] Silver and others (1981); [7] Pushkar and Damon (1974); [8] Livingston (1969); [9] Shakel and others (1977); [10] Swan (1976); [11] Silver (1978).

[2]General References: [12] Volborth (1962); [13] Dexter and others (1983); [14] Kwok (1983); [15] Kwok and Anderson (1983); [16] Volborth (1973); [17] Kessler (1976); [18] Podruski (1979); [19] Krass (1980); [20] J. L. Anderson and others (1979); [21] Davis and others (1980); [22] C. A. Anderson and others (1955); [23] Krieger (1965); [24] Ransome (1903); [25] Keith and others (1980); Banks (1980); [26] Peterson (1938); [27] Schwartz (1953); [28] Creasey (1965); [29] Thorman (1982); [30] Cooper and Silver (1964); [31] Drewes (1968, 1976); [32] Hayes and Raup (1968); [33] this report.

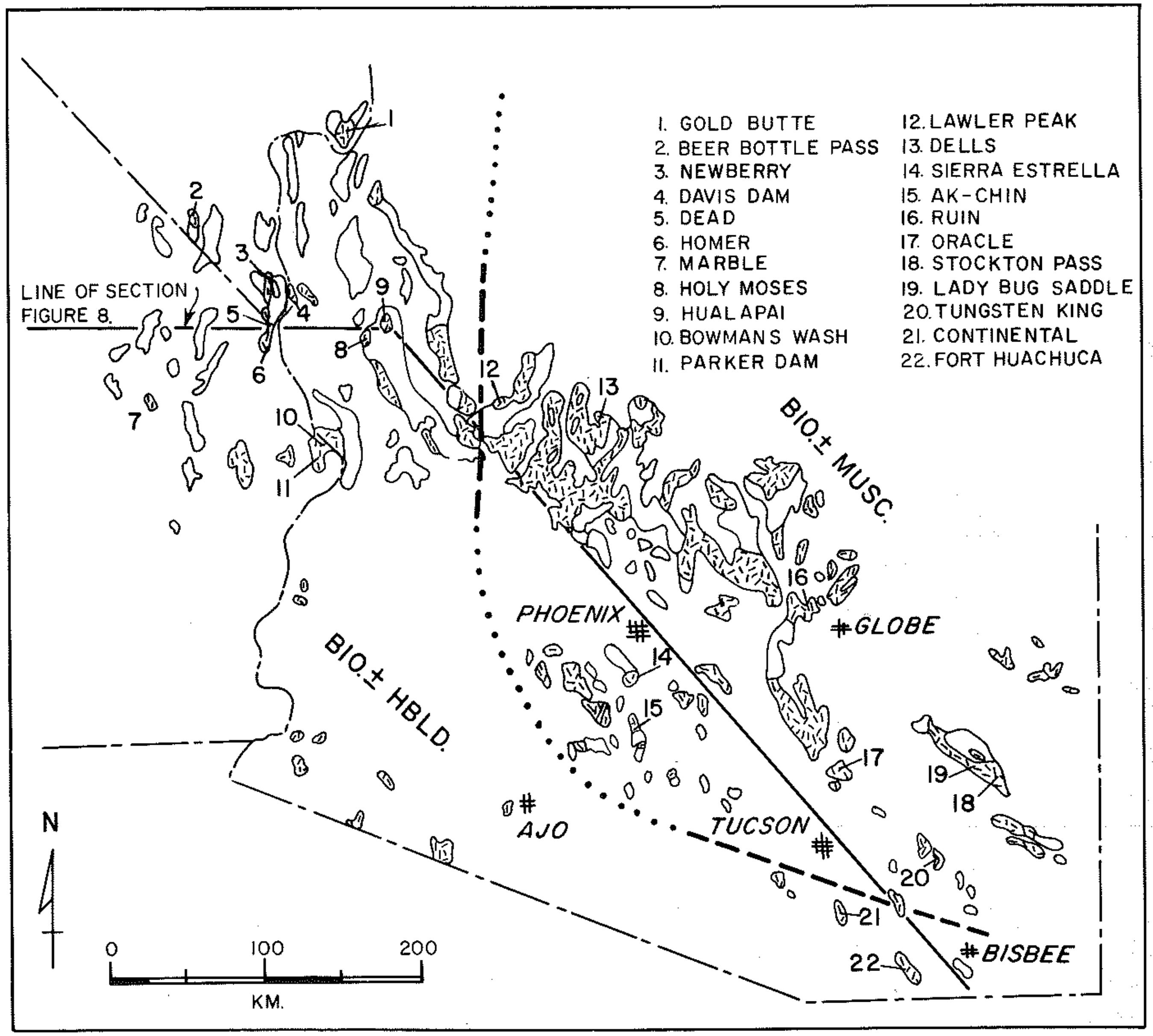

Figure 2. Precambrian outcrop map of Arizona and adjacent California and Nevada. Stippled areas depict granitic intrusions. Numbered localities are of 1.40- to 1.45-Ga granites described in this paper.

including the Sierra Estrella, the Ak-Chin, the Lawler Peak, the Dells, the Ruin, the Oracle, the Stockton Pass, and the Tungsten King granites among others. Together, these granites represent a portion of a peraluminous segment of the transcontinental anorogenic belt that presumably extends up through New Mexico into the Colorado Front Range (J. L. Anderson, 1984; J. L. Anderson and Thomas, 1985). The principal rock type is a porphyritic biotite granite, yet in most cases, muscovite appears subordinate to biotite either throughout the plutonic mass or in the more evolved interior phases. Notably, these granites are not strongly peraluminous, and only the Lawler Peak granite (C. A. Anderson and others, 1955) has a variant that contains muscovite as the sole hydrous phase. Hornblende in these plutons appears to be largely nonexistent. Part of the Ruin and Oracle (Picacho and Tortolita Mountains) granites reportedly contain hornblende (Silver and others, 1980; Banks, 1980), but no hornblende-bearing variants were found in this study, and in general the plutons contain biotite plus subordinate muscovite.

Geographically separate from these moderately peraluminous granites are widespread metaluminous to marginally metaluminous or peraluminous plutons. Residing in southern Arizona, the Fort Huachuca granite and the Continental granodiorite contain biotite plus large distinctive sphene. The latter body also contains occasional amounts of hornblende (Drewes, 1976). Further to the south, the Cananea granite of northern Sonora (T. H. Anderson and Silver, 1977) is apparently a continuation of this same granite type. Mineralogically similar rocks may

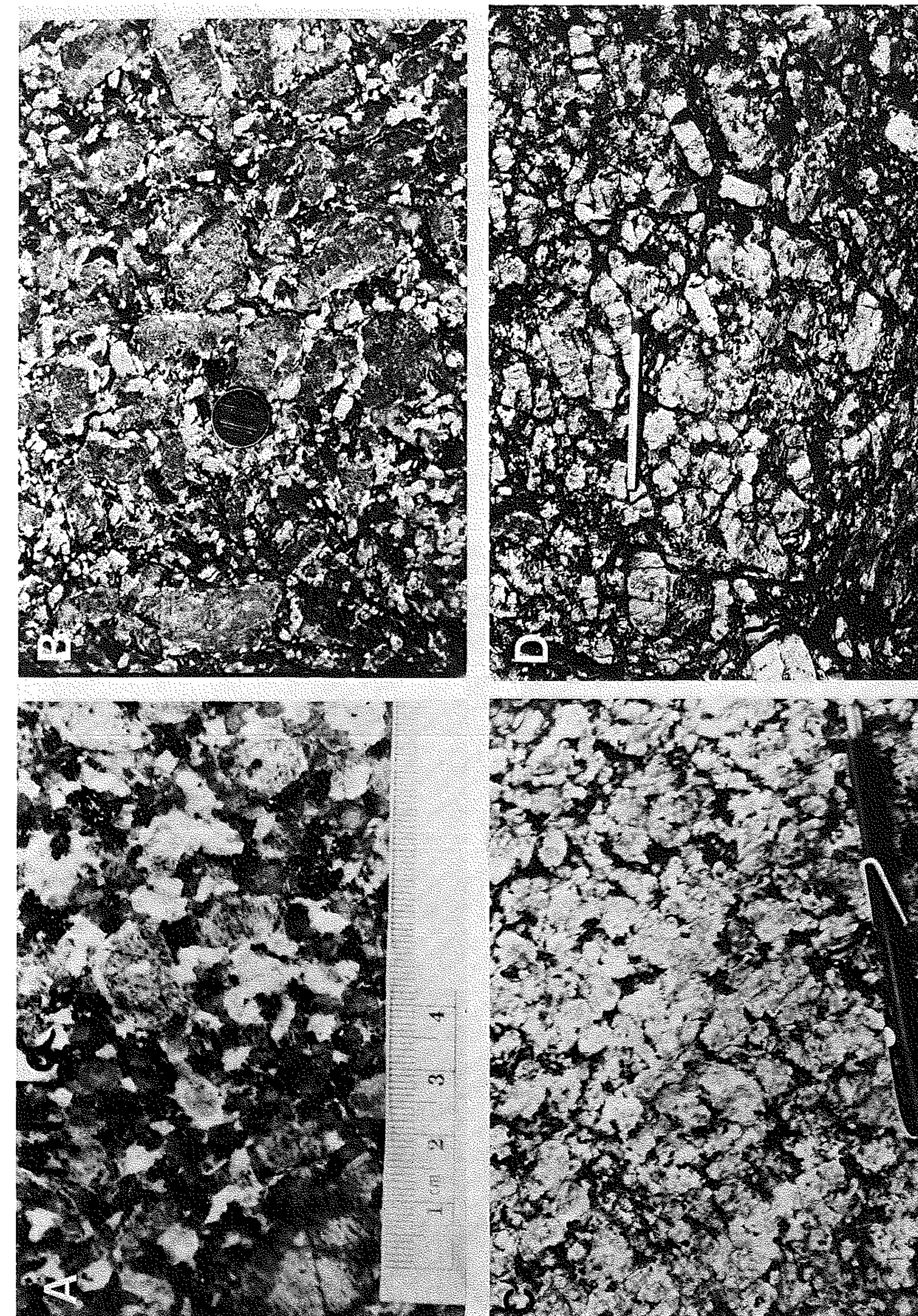

Figure 3. Photographs of representative textural types: A. Gold Butte granite; B. Beer Bottle Pass granite; C. Hualapai granite; D. Parker Dam granite.

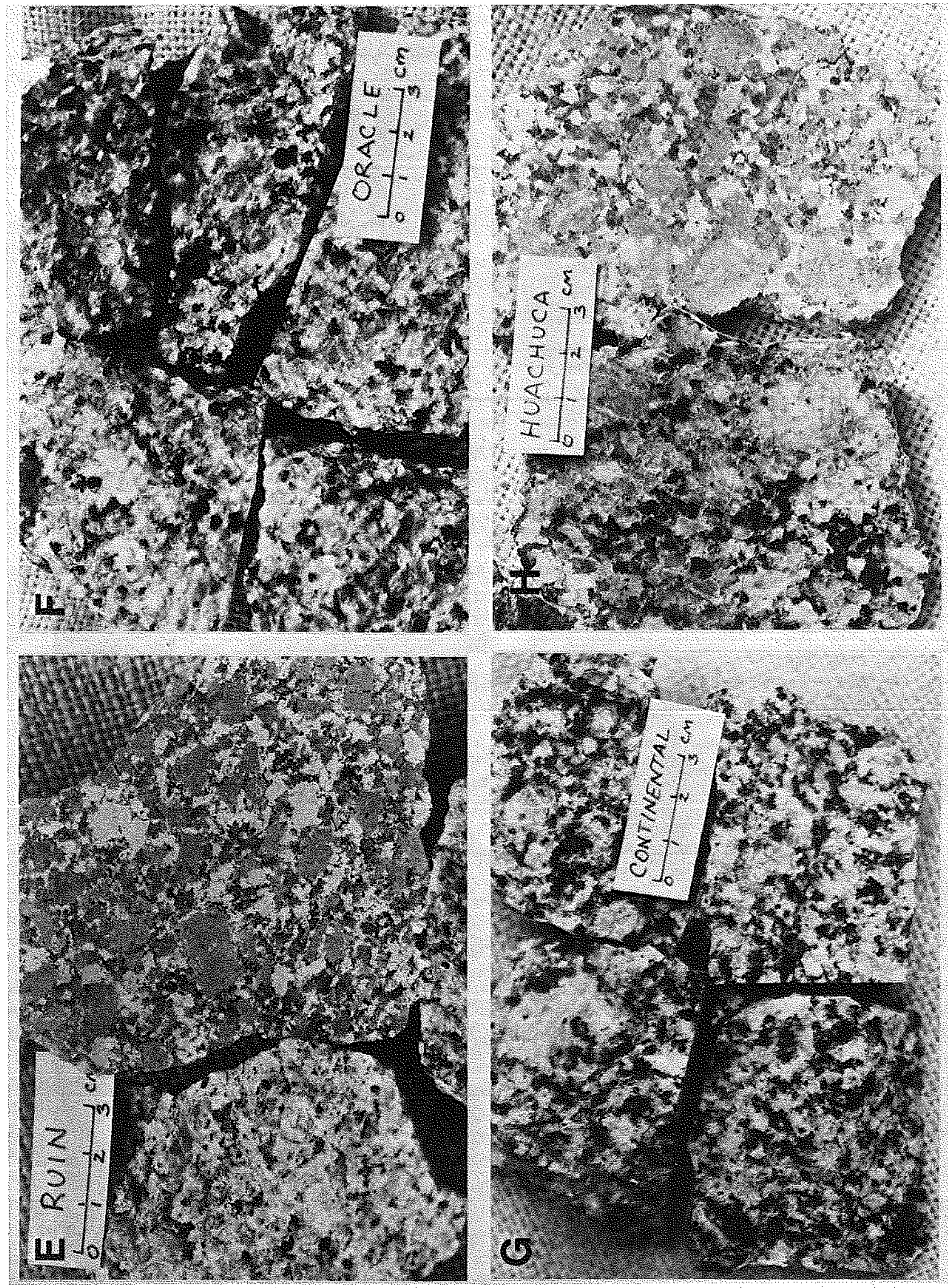

Figure 3, continued. E. Ruin granite; F. Oracle granite; G. Continental granodiorite; H. Fort Huachuca granite.

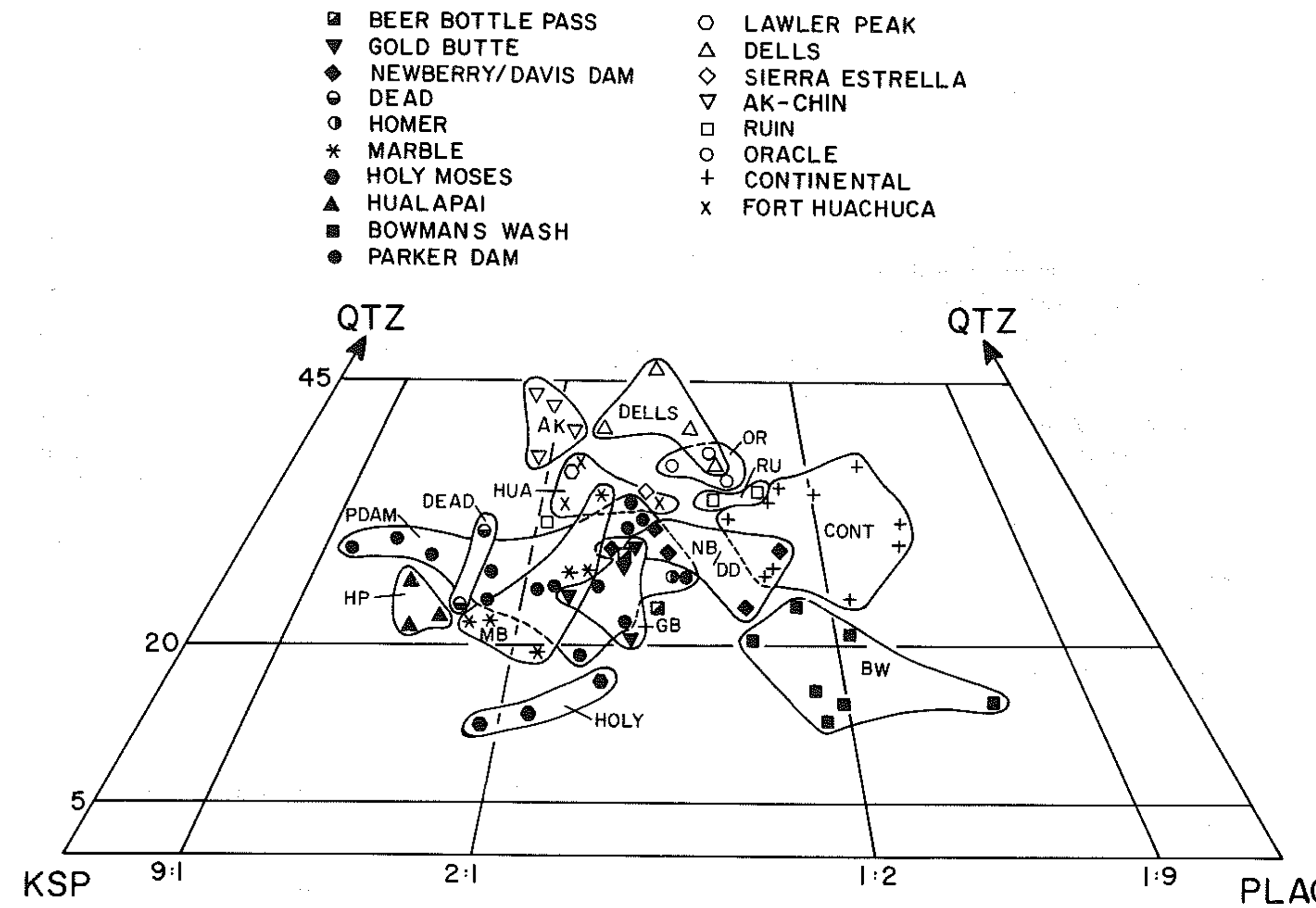

Figure 4. Modal composition in terms of quartz, alkali feldspar, and plagioclase. Sources of data given in table 1.

also comprise inferred 1.4-Ga granites of the Papago Indian Reservation near Ajo, Arizona (M. Grubensky, 1984, personal commun., 1984). To the west, the numerous 1.4-Ga old granites exposed in vicinity of the Colorado River likewise contain only one mica, biotite, plus sphene. Coexisting hornblende occurs in the mafic phases of most, including the Gold Butte, the Beer Bottle Pass, the Newberry, the Holy Moses, the Hualapai, the Bowmans Wash, and the Parker Dam granites. With the exception of a few pegmatites, nowhere are there large bodies of two-mica or muscovite granite, which is a fundamental contrast with 1.4-Ga granites to the east.

Systematic differences between the biotite $\pm$ muscovite and biotite $\pm$ hornblende granites also include the accessory mineralogy. Sphene is common only in the more metaluminous rocks and is usually absent as a primary phase in the peraluminous biotite $\pm$ muscovite granites of Arizona. In its place, monazite is a common accessory mineral (see table 1) as is also the case for similar two-mica granites of Colorado (Anderson and Thomas, 1985). In addition, xenotime occurs in the Ak-Chin and Lawler Peak granites. Although fluorite is a typical late magmatic phase in many anorogenic granites, it is usually absent in the biotite $\pm$ muscovite granites. The Lawler Peak and the Dells plutons are exceptions; however, both are unusually very evolved, highly differentiated granites enriched in many incompatible elements and contain an uncommon assemblage of complementary accessory phases. Fluorite is more common in the Colorado River occurrences including the Gold Butte, Marble, Holy Moses, and Hualapai granites.

COMPOSITIONAL FEATURES

It is important to address the compositional differences between these two contrasting suites of 1.4-Ga granites of the Southwest, but also relevant is how both differ from the remainder of the transcontinental belt and from the older, usually foliated, granitoids that make up a significant portion of their host terrane. By coupling compositional with isotopic constraints, models of the contrasting sources for magma genesis can be formulated.

Like many A-type granites (Wones, 1979), most of these 1.4-Ga granites are potassic, subalkalic, and iron rich (relative to magnesium). Herein lies their fundamental difference with the older Proterozoic granitoids. The older granites are usually calc-alkaline, as evidenced by their greater abundance of Mg, Ca, Na, and Sr and lower Fe/Mg and K (fig. 5), all relative to silica. The 1.4-Ga granites are also enriched in Ti, which from the data at hand (North America, Greenland, and Baltic Shields) seems to be another common attribute of anorogenic potassic granites.

Although the younger Proterozoic granites exhibit a clear compositional affinity to most A-type granites, the biotite ± muscovite suite has lower potassium, higher magnesium, and a lower Fe-Mg ratio (table 2, fig. 5), the latter parameter having some overlap with the calc-alkaline granitoids of the older orogenic suites. They are more peraluminous as shown by higher A-CNK ratios (ratio of molecular Al_2O_3 to $CaO + Na_2O + K_2O$) due principally to lower potassium (table 2). The rocks are also lower in F, Ba, and probably most LIL elements (e.g., REE) if they follow trends of other two-mica, anorogenic suites (Anderson, 1983). Recently completed work on the 1.4-Ga two-mica, sillimanite-bearing Silver Plume and St. Vrain batholiths of Colorado (J. L. Anderson, 1984; J. L. Anderson and Thomas, 1985) indicate a general similarity to these two-mica, anorogenic plutons of Arizona.

Space considerations do not allow a complete perusal of individual variations amongst the numerous anorogenic intrusions in this region. Most can be determined from the data depicted in figure 5 and table 2. Seventy rock analyses were utilized in this study (see Appendix), 52 of which were recently completed by the author or his students (Podruski, 1979; Krass, 1980; Kwok, 1983). In addition, 14 unpublished analyses from the Pinaleno Mountains were provided by Thorman (1984, written commun.). Following the recommendation of S. Keith (1984, personal commun.), omitted in this compilation are data from altered and (or) highly deformed rocks, including about half of the available analyses of the Oracle granite, which had experienced a mid-Tertiary mylonitization and exhibited enrichment in sodium and loss of potassium. Although some of the data for the Continental granodiorite were also excluded, the acceptable analyses exhibit some additional variability which is supportive of the conclusion by Silver (1978) that a portion of the Continental has an age of 1.65 Ga, not 1.44 Ga.

A few plutons merit particular mention. As described by Kwok (1983) and Kwok and Anderson (1983), the Hualapai granite and Gold Butte quartz monzonite are unusual in that both are enriched in alkalies, such that their total K + Na carries them into the alkalic field of Irvine and Baragar (1971). They are not peralkaline, however, just close. For the Hualapai, this compositional feature is enhanced by feldspar accumulation. Similar segregations have been mentioned for the Lawler Peak granite (C. A. Anderson and others, 1955). Consistent with feldspar accumulation, both the Gold Butte and the Hualapai granites are enriched in Ba, the latter also being enriched in Sr.

Certain granites are markedly evolved, representing some form of differentiation from an unexposed parent rock. The Dells and Lawler Peak are siliceous rocks enriched in Rb (and other incompatible elements) and depleted in Ba and Sr. Similar attributes are likewise notable for the Marble, the Ruin, the Sierra Estrella (essentially equivalent chemistry to the Ruin granite), and the Fort Huachuca granites. The Parker Dam granite of the Whipple Mountains exhibits a compositional lineage from 64.7 to 70.0 percent SiO_2. Modeling of that data trend is compatible with fractionation of two feldspars, biotite, and hornblende, the latter mineral apparently responsible for driving the more evolved portion of the Parker Dam granite to a marginally peraluminous composition. The Bowmans Wash quartz monzodiorite, intruded by the Parker Dam granite, is the most mafic of all 1.4-Ga granitoids considered in this survey. Although the pluton lacks pyroxene, its chemistry (low silica, high alkalies) is similar to that of charnockites found elsewhere in the transcontinental belt. Similar plutons, reportedly bearing pyroxene, occur in the Signal area of western Arizona (B. Bryant, personal commun., 1985).

DETAILED MINERALOGY

It was observed above that the major mineralogy of the 1.4-Ga granites of the southwestern United States varies from biotite ± muscovite to biotite-sphene ± hornblende, that all hydrous phases are usually late in crystallization, and that the Fe-Ti oxide mineralogy constitutes a magnetite series. The latter two observations imply low water content and an elevated oxygen fugacity. Thermobarometric calculations are limited for granitic rocks, owing to the underdetermined nature of the phase equilibria. Yet some applications, including two feldspar, biotite-feldspar-magnetite, and muscovite-liquid equilibria, provide some insights. These aspects are developed further below following evaluation of specific mineral composition variations.

Feldspars

The general range of plagioclase composition is given in table 1. For the Colorado River region granites, the feldspar is essentially calcic oligoclase with a typical range of An_{24} to An_{32}. The Newberry, Holy Moses, and Bowmans Wash granites, all less siliceous than the norm, have slightly more calcic plagioclase, up to An_{40}. The Hualapai plagioclase is the most sodic, ranging An_{16} to An_{22}.

Due to the lack of a coexisting calcic phase (e.g., hornblende or sphene), the plagioclase in the peraluminous granites of central and southern Arizona is more calcic, although the normative plagioclase is not, with typical ranges of An_{31} to An_{44}. For the Ruin, Sierra Estrella, Oracle, and Fort Huachuca granites, a second generation of plagioclase, having compositions of An_{21} to An_{24}, occurs as rims adjacent to K-feldspar or as fine-grained crystals. These are presumed to be subsolidus. Primary sodic plagioclase (An_{14} to An_{24}) occurs only in the more evolved granites, including the Ak-Chin, the Lawler Peak, and the Dells.

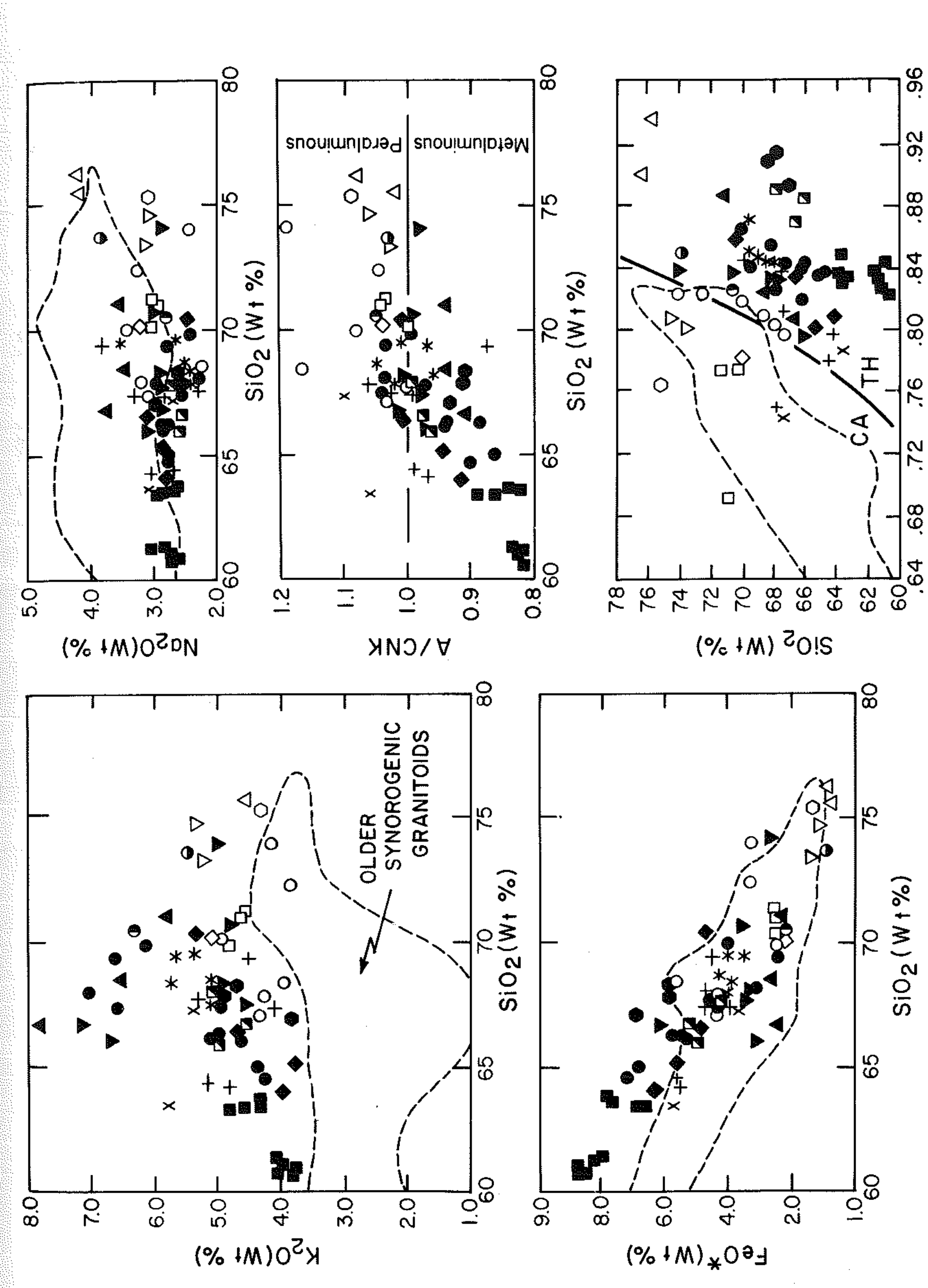

Figure 5. Major- and trace-element composition and comparison to orogenic granitoids of Arizona. Symbols keyed to figure 4. Data for older granitoids from Babcock and others (1979), Krieger (1965), C. A. Anderson and others (1971), and Cooper and Silver (1964). Other data sources given in table 1.

TABLE 2. Average Major and Trace Element Analyses

Pluton	Gold Butte	Beer Bottle	Newberry	Davis Dam	Dead	Homer	Marble	Holy Moses	Hualapai	Bowmans Wash	Parker Dam
No.[1]	6	3	2	2	1	1	5	3	3	9	11
SiO_2	68.86	66.81	64.62	68.43	73.71	70.53	68.78	67.74	68.70	62.17	67.11
TiO_2	.75	1.02	1.30	.75	.19	.40	.61	.89	.41	1.47	.86
Al_2O_3	14.20	14.36	13.98	13.89	13.97	14.45	13.62	12.98	14.31	13.62	14.00
FeO[2]	3.77	4.87	6.03	4.87	.90	2.18	4.02	6.28	2.49	7.97	4.95
MgO	.64	.67	1.47	.91	.16	.49	.71	.60	.49	1.58	.96
MnO	.07	.098	.104	.092	.036	.027	.062	.075	.040	.129	.08
CaO	1.92	2.74	3.46	2.09	.692	1.29	1.92	2.65	1.24	3.96	2.34
Na_2O	2.94	2.69	2.77	2.77	3.83	2.81	2.67	2.68	3.56	2.77	2.69
K_2O	5.51	4.83	3.86	4.98	5.44	6.29	5.35	4.49	6.73	4.18	5.46
LOI	.67		1.16	.71	.58	.61	1.32	.55	.76	1.17	1.03
TOTAL	99.33	98.02	98.75	99.48	99.41	99.08	99.06	99.02	98.74	99.02	99.55
A/CNK[3]	.994	.981	.931	1.012	1.032	1.049	.998	.921	.930	.836	.952
FeO/FeO+MgO	.855	.879	.804	.843	.850	.816	.850	.913	.836	.836	.838
K_2O/Na_2O	1.87	1.79	1.40	1.84	1.42	2.24	2.04	1.70	1.89	1.51	1.93
K_2O+Na_2O	8.45	7.52	6.63	7.75	9.27	9.10	8.02	7.18	10.29	6.95	8.01
Rb[4]	276	191	169	244	89.9	163	422	183	220	138	233
Sr	238	315	278	166	79.8	209	125	132	642	274	186
Ba	2307	1315	1062	814	334	893	678	1038	1300	1392	1111
An/Ab+An[5]	.255	.347	.365	.300	.091	.202	.275	.295	.089	.334	.282
Ref.[6]	13, 14, 33	33	14, 33	14	14	14	14, 33	14, 33	18-20	18-20	18-20

Pluton	Lawler Peak	Dells	Sierra Estrella	Ak-Chin	Ruin	Oracle	Stockton Pass	Ladybug	Contin-ental	Fort Huachuca
No.[1]	1	2	1	2	3	6	9	5	6	2
SiO_2	75.33	75.91	70.15	74.04	70.85	70.02	72.80	68.92	66.78	65.44
TiO_2	.22	.03	.33	.25	.41	.64	.27	.62	.79	.85
Al_2O_3	12.77	13.40	14.38	13.30	13.87	14.14	13.44	13.78	13.87	14.79
FeO[2]	1.35	.76	2.36	1.27	2.51	3.92	1.74	3.48	4.85	4.69
MgO	.42	.08	.66	.31	.73	.92	.48	.66	1.17	1.40
MnO	.07	.03	.082	.075	.08	.10	.04		.11	.12
CaO	1.07	.56	2.11	1.06	1.82	2.05	.88	2.03	2.40	1.65
Na_2O	3.09	4.17	3.20	3.08	2.98	2.90	3.09	2.76	2.98	2.86
K_2O	4.31	4.52	4.85	5.29	4.73	4.20	4.80	5.14	4.44	5.54
LOI	.42	.37			1.06	.74	.85	.61	1.11	
TOTAL	99.05	99.20	98.12	98.68	99.04	99.63	98.58	98.45	98.50	97.34
A/CNK[3]	1.092	1.060	1.002	1.047	1.040	1.089	1.132	.999	.986	1.083
FeO/FeO+MgO	.763	.936	.781	.804	.775	.810	.784	.841	.806	.766
K_2O/Na_2O	1.39	1.08	1.52	1.72	1.59	1.45	1.55	1.86	1.49	1.94
K_2O+Na_2O	7.40	8.69	8.05	8.37	7.71	7.10	7.89	7.90	7.42	8.40
Rb[4]	339	294	190	339	276	185	nd	nd	209	353
Sr	103	11.0	140	57.6	136	165	nd	nd	215	138
Ba	280	25	654	279	491	786	nd	nd	1379	755
An/Ab+An[5]	.161	.069	.267	.159	.253	.282	.118	.288	.286	.242
Ref.[6]	6	6, 23	33	33	6,33	25,33	29	29	31,33	33

[1]Number of analyses averaged
[2]All Fe As FeO
[3]Molecular proportions of $Al_2O_3/(CaO+Na_2O+K_2O)$
[4]Rb, Sr, Ba in ppm
[5]Normative An and Ab
[6]References as in Table 1

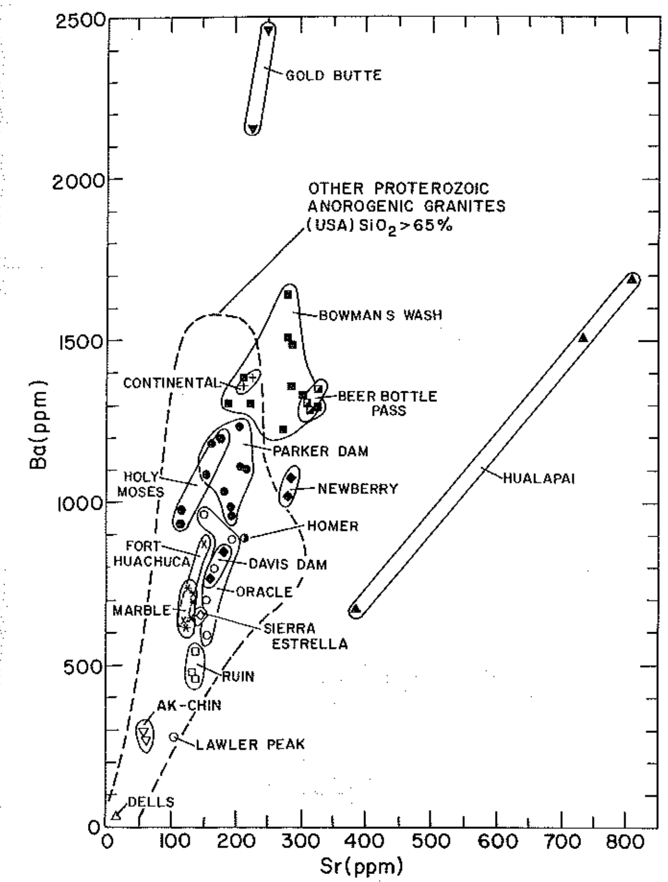

Figure 6. Plot of Ba versus Sr. Symbols keyed to figure 4.

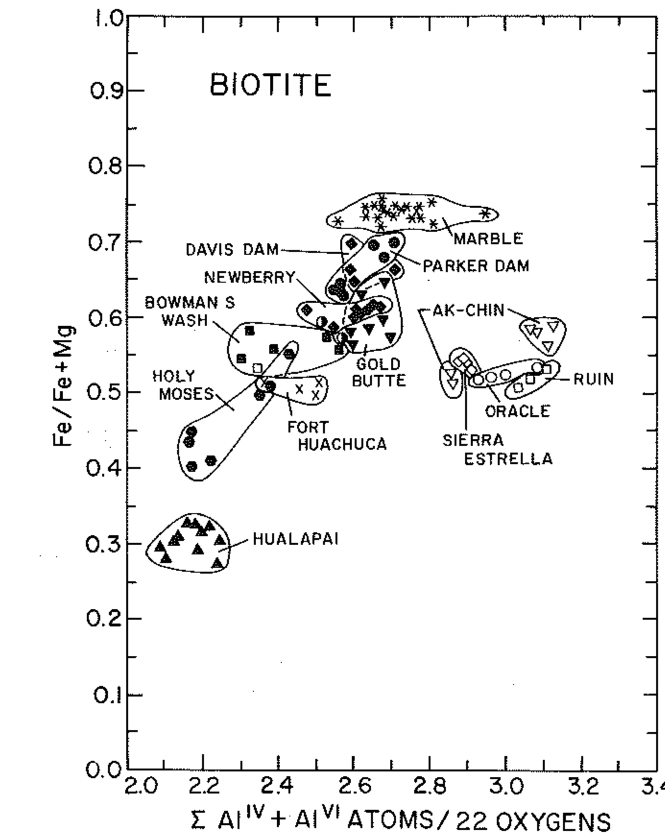

Figure 7. Composition of biotite in terms of Fe/Fe+Mg and total Al (22 oxygens). Sources of data given in table 3. Symbols keyed to figure 4.

The perthitic nature of the K-feldspar required an integrating form of analysis to attain some idea of the primary composition. The Hualapai granite contains the most sodic alkali feldspars, ranging Or_{58} to Or_{71}, which is appropriate from tie-line considerations because the coexisting plagioclase is also sodic. Most compositions fell in the range of Or_{76} to Or_{82}. Only the Newberry, Ak-Chin, and Oracle had more potassic feldspars (range Or_{83} to Or_{87}), which from subsequent thermometry calculations indicates partial subsolidus reequilibration. Expectedly, host compositions of the perthites are quite potassic, ranging from Or_{88} to Or_{92}.

Biotite

Biotite compositions are given in table 3 and figure 7. A significant variation occurs in the aluminous nature of the biotite reflecting the rock composition change from metaluminous (biotite + hornblende) to marginally peraluminous (biotite only) to more strongly peraluminous (two-mica). Hence the more Al-rich biotites occur in the Ak-Chin, Ruin, Sierra Estrella, and Oracle granites.

However, the most profound range in biotite composition lies in the Fe-Fe+Mg ratio. This is unusual. Most ilmenite-series, anorogenic granites have iron-rich biotites with Fe/Fe+Mg from 0.70 to 0.99 (J. L. Anderson, 1983), due principally to a low fO_2 or iron-rich bulk composition, depending on whether or not the mica equilibrated with magnetite. The Fe-Mg ratio of biotite coexisting with K-feldspar and magnetite varies as a function of T, fO_2, and fH_2O (Wones, 1981). The latter two parameters have competing effects; both high fO_2 and low fH_2O drive biotite to Mg-richer compositions. The most iron rich biotite occurs in the Marble granite (Fe/Fe+Mg = 0.72 to 0.75). Biotite from most of the granites have ratios between 0.51 and 0.66. The lowest is in the Holy Moses and the Hualapai granites, the latter have biotite Fe-Fe+Mg ratios as low as 0.27. This is a striking Mg-rich composition that is totally independent of the relatively iron rich composition of the rock. In keeping with its phlogopitic nature, this biotite is very pale green, unlike the brownish green to reddish brown of biotite from the other plutons. The biotites in the Holy Moses and the Hualapai granites are also enriched in fluorine (up to 3.4 wt% F), indicative of the presence of fluorite in these rocks. Biotite in fluorite-absent rocks has a lower, variable fluorine content, usually less than 1.6 wt%.

Amphibole

Hornblende occurs as a primary phase in the Parker Dam, Bowmans Wash, Newberry, Holy Moses, and Hualapai granites. Although late, it generally preceded the initial crystallization of biotite. Its compositional variation complements that of the coexisting biotite, although it

TABLE 3. Average Biotite Analyses[1]

Pluton	Marble	Gold Butte	Newberry	Davis Dam	Holy Moses	Hualapai	Bowmans Wash	Parker Dam	Lawler Peak	Sierra Estrella	Ak-Chin	Ruin	Oracle	Huachuca
No.[2]	23	7	9	5	7	11	6	8	1	4	6	4	4	4
SiO_2	35.58	36.72	36.17	35.32	36.74	39.96	37.35	37.00	36.70	36.40	36.82	35.96	35.62	36.46
TiO_2	3.24	1.28	3.30	2.63	2.36	.65	3.15	2.19	2.10	2.57	2.28	2.66	2.89	3.40
Al_2O_3	14.64	14.70	14.40	14.37	12.75	12.69	13.38	14.90	16.30	16.31	16.99	17.31	16.68	13.77
FeO[3]	27.89	23.62	23.98	25.53	19.61	13.35	23.19	25.54	18.30	20.35	19.69	19.30	19.46	20.32
MgO	5.50	8.90	8.63	7.14	12.64	17.31	10.38	8.06	10.20	9.75	8.62	10.00	9.91	11.06
MnO	.34	.57	.31	.49	.58	.93	.23	.40	1.00	.69	.93	.60	.50	.57
ZnO	.05	.00	.01	.00	.04	.14	.17	.16	nd	.07	.11	.06	.04	.10
CaO	.00	.02	.01	.01	.03	.02	.03	.00	nd	.00	.01	.00	.00	.00
Na_2O	.10	.07	.08	.08	.16	.07	.08	.07	nd	.05	.02	.03	.09	.10
K_2O	9.18	9.12	9.45	9.34	9.52	9.78	9.43	9.44	10.40	10.08	9.68	10.01	9.84	9.55
F	.38	1.65	.94	1.51	2.86	3.11	1.93	2.07	1.30	1.19	1.46	.80	.98	1.68
Cl	28	.10	.13	.16	.17	.08	.14	.20	nd	.01	.02	.01	.03	.02
TOTAL	96.99	96.22	97.03	96.02	96.36	96.77	98.62	98.11	96.1	96.95	95.85	96.39	95.63	96.36
						Formula per 22 Oxygens								
Si	5.569	5.631	5.539	5.512	5.526	5.764	5.568	5.537	5.552	5.482	5.555	5.426	5.422	5.521
Al^{iv}	2.431	2.369	2.461	2.488	2.261	2.159	2.351	2.463	2.448	2.518	2.445	2.574	2.578	2.458
Al^{vi}	.270	.289	.138	.155	.000	.000	.000	.166	.459	.378	.577	.505	.416	.000
Ti	.381	.148	.380	.309	.267	.071	.353	.246	.239	.291	.259	.302	.331	.387
Fe	3.651	3.029	3.071	3.332	2.467	1.611	2.891	3.197	2.315	2.563	2.484	2.435	2.477	2.573
Mg	1.283	2.034	1.969	1.660	2.833	3.721	2.306	1.798	2.300	2.188	1.938	2.249	2.248	2.496
Mn	.045	.074	.040	.065	.074	.114	.029	.051	.128	.088	.119	.077	.064	.073
Zn	.006	.000	.001	.000	.004	.015	.019	.018	.000	.008	.012	.007	.004	.011
Ca	.000	.003	.002	.002	.005	.003	.005	.000	.000	.000	.002	.000	.000	.000
Na	.030	.021	.024	.024	.047	.020	.023	.020	.000	.015	.006	.009	.027	.029
K	1.833	1.784	1.846	1.859	1.827	1.800	1.793	1.802	2.007	1.937	1.863	1.925	1.911	1.845
F	.188	.800	.455	.745	1.361	1.419	.910	.980	.622	.567	.697	.382	.472	.805
Cl	.074	.026	.034	.042	.043	.020	.035	.051	.000	.005	.005	.003	.008	.005
ΣVI	5.636	5.574	5.600	5.521	5.433	5.454	5.518	5.475	5.441	5.517	5.389	5.574	5.541	5.520
Fe/Fe+Mg	.740	.598	.609	.667	.465	.302	.556	.640	.502	.539	.562	.520	.524	.508

[1]Marble, Gold Butte, Newberry, David Dam, Holy Moses, Hualapai data from Kwok (1983); Lawler Peak data from Silver and others (1981); Bowmans Wash, Parker Dam, Sierra Estrella, Ak-Chin, Ruin, Oracle, Huachuca from J. L. Anderson (unpublished data).
[2]Number of analyses averaged.
[3]All Fe as FeO.

TABLE 4. Average Hornblende Analyses[1]

Pluton	Newberry	Holy Moses	Hualapai	Bowmans Wash	Parker Dam
No.[2]	8	4	6	9	4
SiO_2	40.72	39.82	43.96	41.46	39.56
TiO_2	1.38	1.35	.55	1.43	1.18
Al_2O_3	10.59	10.12	8.04	10.31	10.67
FeO[3]	23.69	23.77	19.26	23.40	26.17
MgO	5.98	6.13	9.88	6.88	4.96
MnO	.61	.87	.97	.52	.59
CuO	11.13	11.34	10.87	10.48	11.11
Na_2O	1.40	1.76	1.63	1.58	1.63
K_2O	1.70	1.75	1.62	1.56	1.84
F	.78	1.33	1.26	.63	.86
Cl	.24	.00	.11	.13	.25
TOTAL	97.84	97.68	97.59	98.09	98.40
		Formula per 23 oxygens			
Si	6.359	6.256	6.697	6.424	6.242
Al^{iv}	1.641	1.744	1.303	1.576	1.758
Al^{vi}	.308	.130	.142	.308	.227
Ti	.162	.160	.063	.167	.140
Fe	3.094	3.123	2.454	3.032	3.453
Mg	1.392	1.435	2.243	1.589	1.163
Mn	.081	.116	.125	.068	.079
Ca	1.862	1.909	1.774	1.740	1.878
Na	.424	.536	.482	.475	.499
K	.339	.351	.315	.308	.370
F	.385	.661	.607	.309	.429
Cl	.064	.000	.028	.034	.067
Fe/Fe+Mg	.690	.685	.522	.656	.748

[1]Newberry, Holy Moses, Hualapai data from Kwok (1983) and Bowmans Wash and Parker Dam from J. L. Anderson (unpublished data).
[2]Number of analyses averaged.
[3]All Fe as FeO.

always has a higher Fe-Fe+Mg ratio (table 4). Following the classification of Leake (1978), this amphibole ranges from hastingsite to hastingsitic hornblende. An exception is the Hualapai hornblende which is ferroedenitic based on its more Mg-rich, Al-poor composition.

Muscovite

As explained by J.L. Anderson and Rowley (1981) and Miller and others, (1981), plutonic muscovite is far from ideal in composition. The primary muscovites in the Oracle, Ruin, Ak-Chin, Lawler Peak, and Sierra Estrella granites are no exception. Their higher Si, Fe and Mg and lower Al relative to ideal muscovite is due to a high, yet typical celadonite content.

The mole percentage of muscovite is limited to 54.5 to 65.8 and the mole percentage of celadonite (principally the end member $KMgAlSi_4O_{10}(OH)_2$) ranges from 13.2 to 23.4. Charge balance considerations require most of the iron to be ferric, which is represented in table 5 as ferrimuscovite (XFe). Characteristic of primary plutonic muscovite is a high titanium content, which in these rocks ranges up to 1.5 wt percent TiO_2. Secondary muscovite (sericite) occurs as well but can be discerned not only from its texture (always on feldspar) but also from its much lower titanium content (see table 5).

TABLE 5. Average Muscovite Analyses[1]

Pluton	Lawler Peak	Sierra Estrella	Ak-Chin	Ruin	Oracle	Ak-Chin Sericite
No.[1]	1	4	6	3	4	2
SiO_2	46.50	46.90	46.80	46.55	47.51	46.69
TiO_2	.70	1.08	1.03	1.52	.56	.07
Al_2O_3	28.20	30.06	29.21	32.04	28.85	32.27
FeO	5.60	5.14	5.16	4.97	5.57	3.93
MgO	2.20	1.70	1.89	1.19	2.27	.94
MnO	.20	.07	.11	.04	.05	.05
ZnO	.00	.04	.06	.01	.02	.01
CaO	.00	.01	.00	.01	.01	.01
Na_2O	.20	.04	.14	.04	.06	.12
K_2O	10.90	8.86	10.10	8.08	9.46	9.64
F	.60	.34	.85	.29	.39	.28
Cl	.00	.01	.01	.01	.01	.01
TOTAL	94.85	94.08	94.92	94.64	94.58	93.88
		Formula per 6 Octahedral + tetrahedral cations				
Si	3.156	3.124	3.145	3.054	3.166	3.129
Al^{iv}	.844	.876	.855	.946	.834	.871
Al^{vi}	1.412	1.485	1.459	1.533	1.432	1.679
Ti	.036	.054	.052	.075	.028	.004
Fe	.318	.286	.290	.273	.310	.220
Mg	.223	.169	.189	.116	.225	.094
Mn	.011	.004	.006	.002	.003	.003
Zn	.000	.002	.003	.000	.001	.000
Ca	.000	.001	.000	.001	.001	.001
Na	.026	.005	.018	.005	.008	.016
K	.944	.753	.866	.676	.804	.824
F	.129	.072	.181	.060	.082	.059
Cl	.000	.001	.001	.001	.001	.001
CHG	21.740	21.548	21.774	21.480	21.552	21.718
Fe/Fe+Mg	.588	.629	.605	.701	.579	.701
XMu[4]	.545	.620	.587	.658	.580	.754
XPg	.026	.005	.018	.005	.008	.016
XCe	.234	.180	.198	.132	.229	.135
XTi	.036	.054	.052	.075	.028	.004
XFe	.159	.141	.145	.130	.155	.091

[1]Lawler Peak data from Silver and others (1981), remainder from J. L. Anderson (unpublished data).
[2]Number of analyses averaged.
[3]All Fe as FeO.
[4]Mole fraction of end members muscovite, paragonite, celadonite ($K(Mg,Fe)AlSi_4O_{10}(OH)_2$), a titaniferous species ($KTiAlSi_3Al_2O_{10}(OH)_2$), and ferrimuscovite ($KFe_2Si_3AlO_{10}(OH)_2$), respectively.

Fe-Ti Oxides

Magnetite, the predominant if not the sole Fe-Ti oxide in these rocks, began to crystallize after the feldspars and quartz but before the hydrous silicates. Unfortunately, its present composition, found to be nearly pure Fe_3O_4 (a common consequence of subsolidus reequilibration in plutonic rocks), precluded any thermobarometic applications. Minor ilmenite was found in several of the granites, including the Parker Dam, Bowmans Wash, Newberry, Davis Dam, Oracle, Ruin, Ak-Chin, Sierra Estrella, and Fort Huachuca granites. The mole fraction ratios of $X_{ILM}/(X_{HEM} + X_{ILM})$ generally fall in the range of 0.93 to 0.99 but the substitution of a $MnTiO_3$ component is high, from 12 to 22 mole percent (or 5.5 to 13.1 wt percent MnO). In the

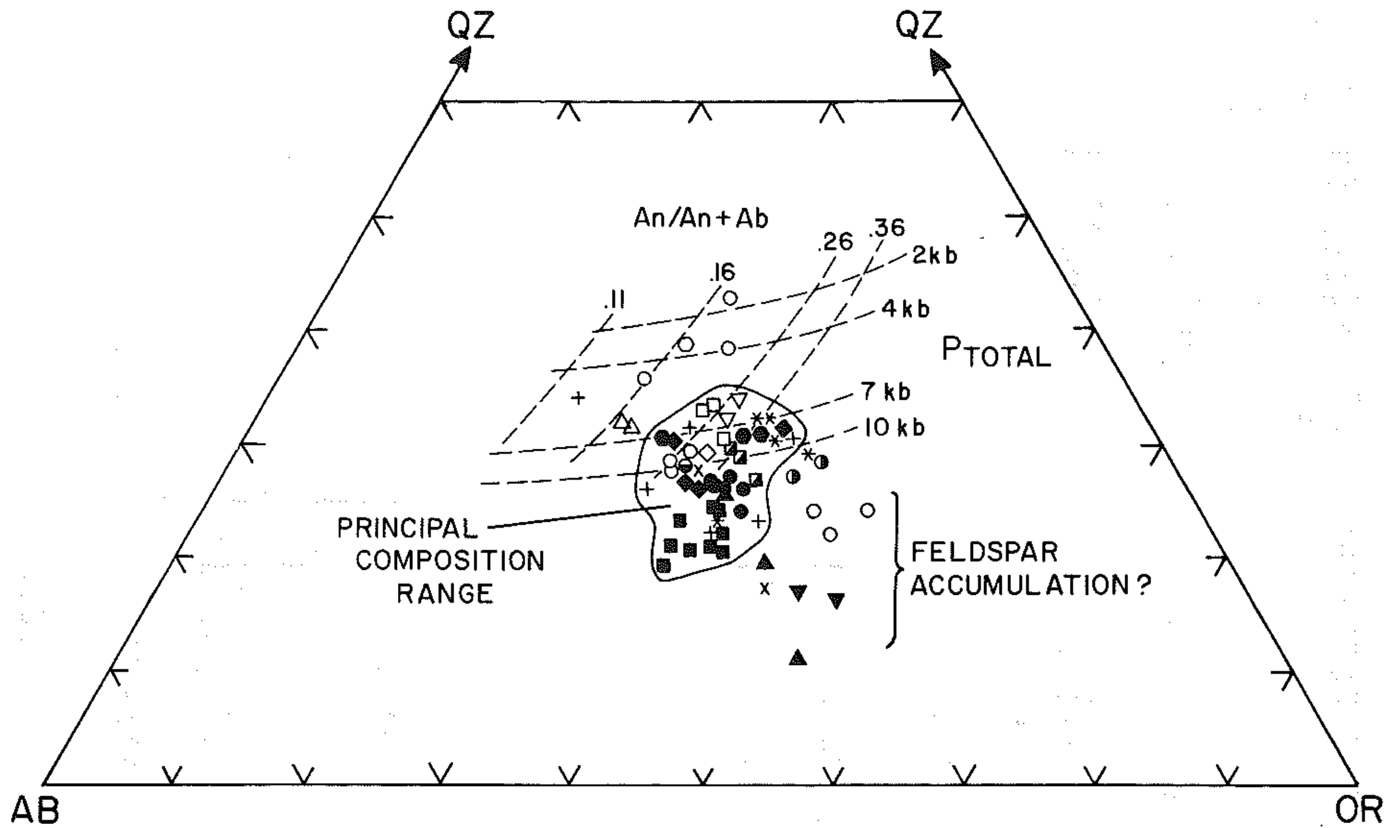

Figure 8. Normative quartz, albite, and orthoclase compositon and comparison to experimental minimum melt data. Symbols keyed to figure 4.

Parker Dam and Bowmans Wash granites, the ilmenite is commonly altered to a ferropseudobrookite-pseudobrookite composition.

PHYSICAL CONDITIONS

Depth of Magma Generation

Barometric calculations for rocks of granitic composition are crude at best. One approach is comparison to water-saturated minima in the granite system. If sufficient data exist to constrain the parental or most primitive composition, an estimate of the depth of melting can be inferred if the magma has experienced minimal changes in composition since melt generation. Such applications for plutonic rocks are fraught with assumptions including whether the rock represents minimum or near minimum melt. However, the effects of subsaturation water contents are minimized because the lowering of P_{H_2O} relative to P_{total} appears to shift minimum melts in a path subparallel to the isobars. Fluorine is more problematic (shifts melts toward the Ab corner in the Qz-Ab-Or system) but most of the more primitive members are not particularly fluorine rich (except the Holy Moses and Hualapai granites). Despite these considerations, most of the Proterozoic anorogenic granites of the North American continent fall near the 7 to 10 kb minima, implying a middle to lower crustal source (J. L. Anderson, 1983). As depicted in figure 8 the granites of the southwestern United States yield a similar result, yet a general separation of data for the peraluminous and metaluminous granites suggests that the latter plutons may have originated at a slightly deeper crustal level. Several samples have compositions that fall outside the principal range which can be accounted for by differentiation (Dells, Lawler Peak, portions of the Oracle granites) or alkali feldspar accumulation (Parker Dam, Hualapai, Gold Butte, Oracle, and Fort Huachuca granites).

Depth of Emplacement

Barometric estimates for the level of emplacement of these plutons are not yet definitive. The epizonal nature of the individual intrusions indicate that shallow crust depths would be reasonable. However, none of these magma systems was emplaced sufficiently shallow to yield eruptive centers. J. L. Anderson and Rowley (1981) have argued that plutonic muscovite, corrected for titaniferous and celadonitic components, lowers the minimum pressure (down from 4.0 kb) at which this phase can coexist with granitic liquid. For the muscovite-bearing plutons (Oracle, Ruin, Sierra Estrella, Ak-Chin, and Lawler Peak), a preliminary minimum estimate is 2.7 to 3.2 kb.

The composition of hornblende apparently is also depth dependent, and Hammarstrom and Zen (1985) have suggested that total Al (atoms per 23 oxygens) increases

with pressure according to the expression

$$P(kb) = 5.04\ (Al^{iv} + Al^{vi}) - 3.89$$

This barometer has special application to the hornblende-bearing plutons of the Colorado River region (Parker Dam, Bowmans Wash, Newberry, Holy Moses, and Hualapai), which have total Al ranging from 1.37 to 1.98 atoms (table 4). The corresponding pressure estimates range from 3 to 6 kb, which is too large a spread to be geologically reasonable. However, analysis of this data set (table 4) and that for many other hornblendes in granitic rocks (E. Young, personal commun., 1985; J. L. Anderson, unpublished data), show a positive Fe/Mg effect on total Al. Hence, calculated pressures on more iron rich amphiboles should lead to erroneously high values. The Hualapai hornblendes have the most intermediate Fe/Mg (Fe/Fe+Mg = 0.52) and the calculated pressure of 3.5 kb is perhaps the most reasonable.

Independent estimates of pressure can be derived from barometric calculations for host rock mineral assemblages, whether of contact metamorphism or preceding regional metamorphism. Couch (1981) has calculated 3.0 to 3.7 kb (11.1 to 13.7 km) for a garnet-biotite-cordierite-sillimanite-feldspar assemblage in a contact aureole adjacent to a suspected 1.4-Ga-old pluton in the eastern McDowell Mountains. More recently, Thomas and other (in press) have evaluated the circa 1.7-Ga regional metamorphic conditions in high amphibolite to granulite terranes of the Colorado River region. Barometer calculations range from 2.2 to 4.5 kb (8.1 to 16.7 km), which serve as a minimum pressure (depth) estimate being that they characterize crustal levels some 300 Ma prior to intrusion of the anorogenic event.

Crystallization Temperature

Using 3 kb as a minimum pressure, feldspar thermometry calculations (formulation of Hazelton and others, 1982) resulted in the following minimum temperatures: Hualapai: 732-794°C, Marble: 616-759°C, Gold Butte: 615-632°C, Bowmans Wash: 625-659°C; Parker Dam: 616-661°C; Dead Mountains: 606-627°C; Ruin: 701-703°C; Fort Huachuca: 649-725°C; and Sierra Estrella: 622-647°C. The Ak-Chin, Oracle, and Newberry granites yielded lower results (540-590°C), perhaps the result of reequilibration. Overall, the metaluminous granites appear to have crystallized at higher temperatures. The lower temperatures for the peraluminous suite may reflect higher water contents as previously inferred from the fact that some, not all, are associated with late-stage pegmatites.

Oxygen Fugacity

In general, the above temperature estimates are fairly uniform. However, the most dramatic intensive parameter variation rests with the level of oxygen fugacity (fO_2), which appears to range over three magnitudes. Previously described is the Fe/Fe+Mg of biotite which ranges from 0.76 (Marble) to 0.28 (Hualapai). This range of fO_2 far

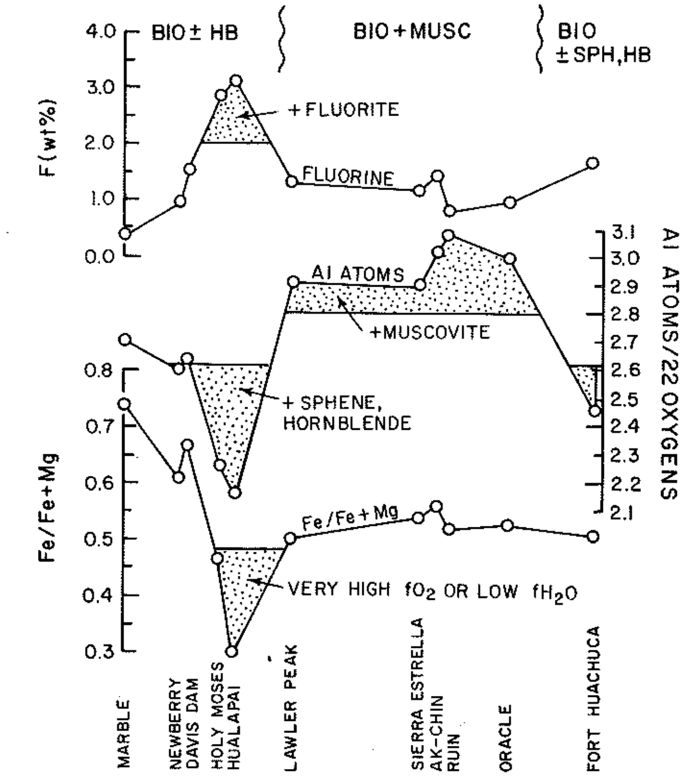

Figure 9. Regional variations in biotite composition from California to southeastern Arizona. Transect depicted in figure 2.

surpasses the effect of variable fH_2O and must relate to a marked increase in fO_2 geographically coincident with the Hualapai Mountains region. Figure 9 depicts the compositional change of biotite on a generally northwest-southeast transect across Arizona into eastern California. The changes in alumina and fluorine are depicted, but most important are the relative proportions of Fe to Mg.

Assuming a maximum P_{H_2O} range of 2 to 4 kb, the calculated biotite stability contours are shown in figure 10. Biotite of the Marble granite apparently crystallized under the more reducing conditions ($10^{-16.3}$ bars at 700°C; near the QFM buffer). Most of the other granites appear to have crystallized with fO_2 In the range of $10^{-15.8}$ to $10^{-14.9}$ bars. The fO_2 for the Holy Moses granite runs higher, and that for the Hualapai granite indicates crystallization under even more oxidizing conditions, relative to plutons both to the east and west. At 700°C, the estimate is $10^{-13.4}$ bars. As noted by Kwok (1983) and Kwok and Anderson (1983), this granite crystallized under unusually high oxidizing conditions, unmatched elsewhere in the transcontinental belt. Although the level of oxidation can change during rise and emplacement of a granitic magma, the uniformity of existing data for the Hualapai granite indicates that this fO_2 is an imprint of a generously oxidized source. It is notable that the pluton generates a significant positive anomaly on the aeromagnetic map of Arizona (Sauck and Sumner, 1970).

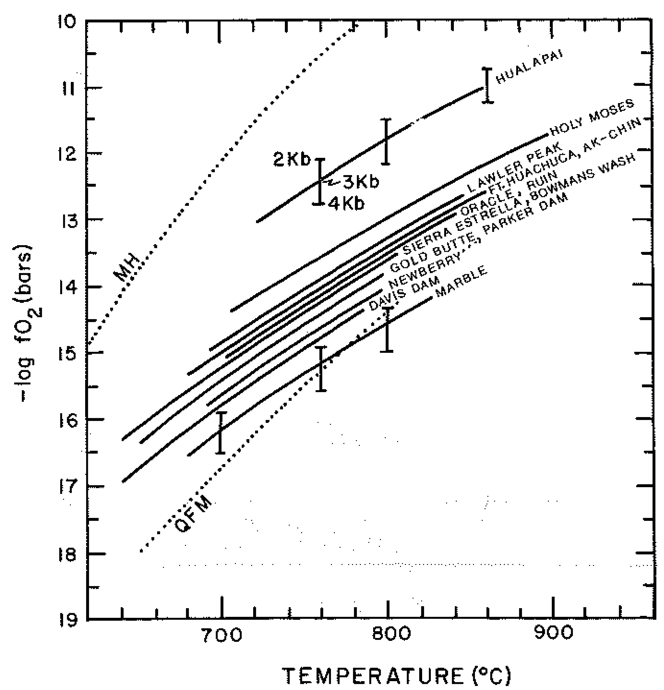

Figure 10. Contours of biotite stability at P_{H_2O} of 3 kb. Error brackets for a P_{H_2O} of 2 and 4 kilobars given for uppermost and lowermost contours. MH = magnetite-hematite buffer. QFM = quartz-fayalite-magnetite buffer.

The magnetite and ilmenite of all rocks studied have compositions too near their ideal end-members to reflect magmatic conditions. As is common for plutonic rocks (Lindsley, 1976), subsolidus reequilibration during slow cooling apparently led to a simultaneous oxidation of the magnetite and reduction of ilmenite involving the exchange mechanism $Fe^{2+}+Ti = 2Fe^{3+}$ (without necessary gain or loss of oxygen). This is a consequence of a T-fO_2 cooling path that bisects the nonparallel stability isopleths for the two phases.

SOURCE MATERIAL

The previous section outlined how the general major-element composition of these granites is consistent with partial melting of a crustal source at depths of 25 to 37 km or greater. Work on similar rocks of the same age (J. L. Anderson and Cullers, 1978; Cullers and others, 1981; Condie, 1978) has shown that the REE composition is likewise compatible with a crustal source, one of quartz dioritic to granodioritic composition, either metaplutonic or metavolcanic, with a variable proportion of metasedimentary component. The latter is particularly relevant for the more peraluminous granites of central and southeastern Arizona.

There is not a lot of initial Sr isotope data for these rocks (table 1), but they show general conformity with that for the rest of the transcontinental belt (J. L. Anderson, 1983), which has an average initial Sr isotopic ratio of 0.7051±.0025(1σ). The indication is a source neither very radiogenic nor too old. This conclusion has recently been confirmed by the Nd-Sm studies of Bennett and DePaolo (1984), who concluded a crustal source for several granites in the vicinity of the Colorado River (including the Parker Dam, Hualapai, Davis Dam, and Gold Butte granites) and for others in central and southeastern Arizona. Likewise, Nelson and DePaolo (1985) and Farmer and DePaolo (1984) have studied the Marble, Oracle, Dells, and Lawler Peak granites with similar conclusions. For most of these plutons, the ϵ_{Nd} values are strongly negative and indicate a crustal source, largely, if not exclusively, Proterozoic, which formed from the mantle some 250 to 400 Ma earlier.

The physical state of an anorogenic crustal source has attracted differing forms of speculation. To account for the relatively dry nature of anorogenic granites, Chappell (1979), Loiselle and Wones (1979), and Collins and others (1982) suggested that the source be a residue from an earlier melting episode (hence, their R-type granite). However, such a refractory source would be depleted in silica and fluorine, as well as water and many incompatible elements. Moreover, Bennett (1984, personal commun.), has suggested that her Nd-Sm data preclude the R-type origin. A high-grade metaigneous to metasedimentary source, stripped of most of its available water during preceding orogenic metamorphism, is consistent with a range of isotopic and geochemical data. For example, a tonalitic metaigneous source has a water budget far less than one percent, part of which will be retained during melting. An additional attribute of this type of source is that the degree of melting will be limited, a consequence of the large ΔT for the solidus and liquidus of a relatively dry crustal source and the ultimate cause of the potassic and iron- and fluorine-rich nature of these granites.

This general model for the granitic magmas of the transcontinental belt must be, of course, tempered for intrabelt regional variations. The peraluminous segment from Colorado to central and southeastern Arizona exhibits some differences additional to higher A-CNK ratios. The most straightforward explanation is that the increased contribution of a metasedimentary component will provide a higher water budget, which leads to large degrees of partial melting. Qualitatively, this will dilute the concentration of alkalies, fluorine, and most LIL elements and lower the Fe-Mg ratio.

MAGMATIC AND METAMORPHIC VARIATIONS OF THE HOST TERRANES

The most apparent mineralogic variation of the 1.4-Ga granites is the biotite ± hornblende to biotite ± muscovite transition that presumably results from a physical change in the crustal source. The transition boundary, still subject to revision, is, on its western extent, proximal to dramatic change in the estimated levels of oxygen fugacity of the magmas and presumably their source.

There are three other indications that the western transition boundary is even more fundamental. For one, it

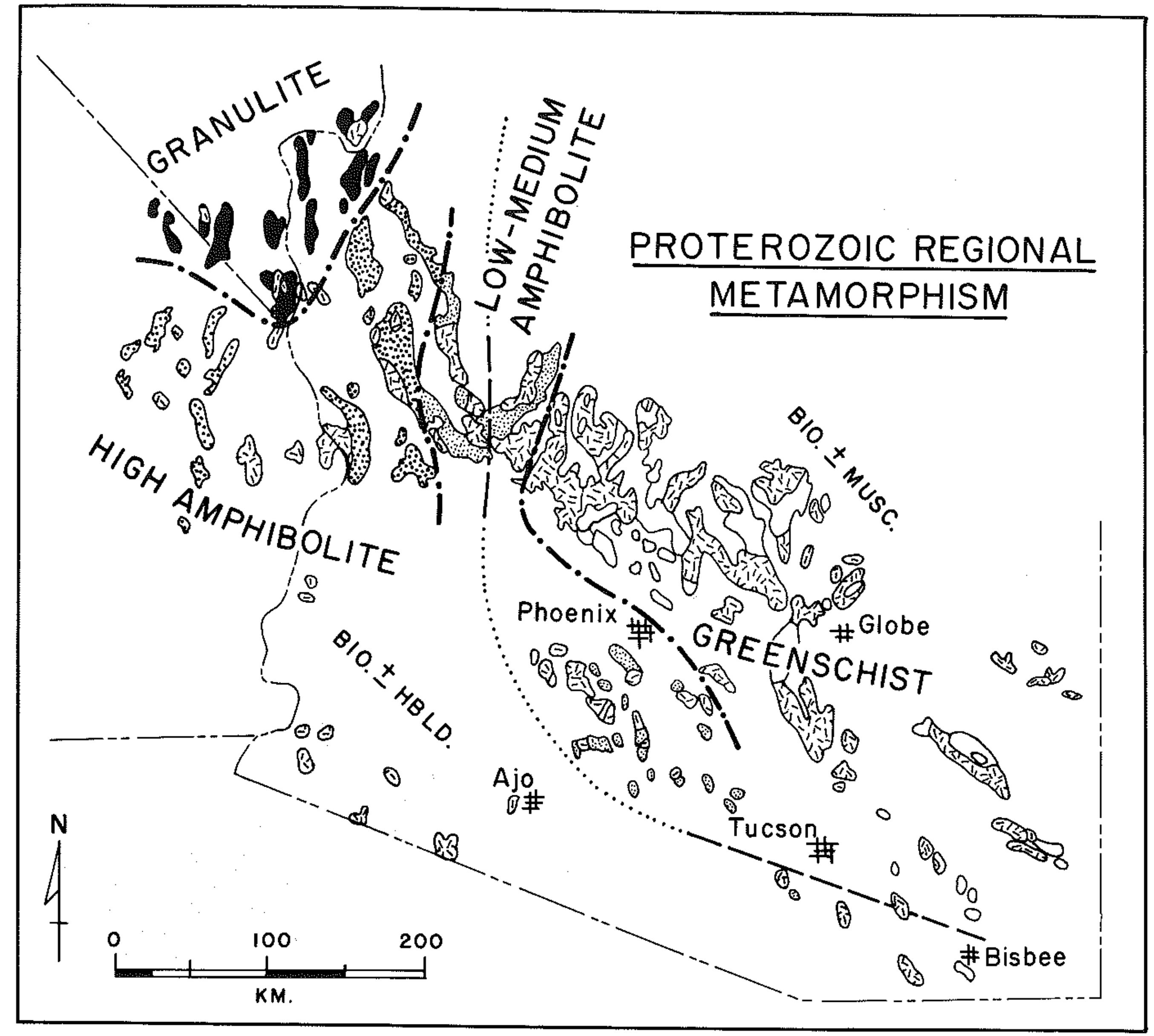

Figure 11. Early Proterozoic metamorphic terranes of the southwestern United States. This compilation, still imprecise, draws from the description of several workers, including Ransome (1903), C. A. Anderson and others (1955), Krieger (1965), Volborth (1962, 1973), Podruski (1979), Davis and others (1980), Thorpe (1980), Couch (1981), Sommer (1982), and Thomas and others (in press). The heavy dash-dot lines depict approximate changes in metamorphic grade but are not isograds as the age of the metamorphism ranges in age from about 1.75 Ga (west) to 1.65 Ga (east) (Silver, 1968). The light dash and dotted curve represents the change of granite type at 1.4 Ga. Areas affected by major Mesozoic and Tertiary metamorphism have been omitted.

is closely coincident to a major change in metamorphic grade of the host lithologic units. The regional variations in metamorphic grade are shown in figure 11; however, the data are imprecise and this compilation must be viewed as preliminary. The metamorphism is of variable age, and contact effects due to later Proterozoic granitic intrusion have yet to be well documented. For many areas, the grade of metamorphism has simply not been studied and will be a difficult task where there is a strong overprint of Mesozoic to Tertiary plutonism and deformation. However, the general trends clearly indicate that the older host rocks to the east are of lower metamorphic grade, including the greenschist-grade Pinal Schist and the upper greenschist- to low- and medium-amphibolite-grade Yavapai Series. To the west, the older units are all high-grade quartz feldspathic gneisses, with peak metamorphism at upper amphibolite grade (K-feldspar sillimanite zone) in western Arizona and adjacent California increasing northward to low granulite grade in southern Nevada (Thomas and others, in press).

A second change deals with the compositional nature of the older foliated granitoids. Those in the lower grade metamorphic terranes in central Arizona are typically calc-alkaline, although a few, usually late to postkinematic, are potassic. Rock types include the range from quartz diorite to granodiorite. In contrast, the calc-alkaline granitoids appear to be insignificant in number, if not absent, in the high-grade metamorphic region to the west. Some plutons have U-Pb (zircon) ages as old as 1.74 Ga (J. L. Anderson and J. Wright, in prep.) yet are potassic and, in fact, similar in many respects to the 1.4-Ga-old anorogenic suite.

Thirdly, the western transition boundary is strikingly similar to the crust formation province boundary of Bennett and DePaolo (1984). Based on Nd model ages of 1.4-Ga and older granites, their boundary separates an eastern province having T_{DM} ages of 1. 7 to 1.8 Ga from a western province with T_{DM} ages of 1.8 to 2.0 Ga. Further to the west, a third province having T_{DM} of 2.0 to 2.3 Ga resides in southeastern California. Bennett and DePaolo noted that these provinces may delineate either aging of, or an increased Archean component in, the lower crust, from which these 1.4-Ga-old granites were derived. Clearly, these variations in Nd isotopic signature are coincident with fundamental changes in granite type and the preceding thermal history of the crust.

TECTONIC SIGNIFICANCE

The origin of the transcontinental anorogenic belt remains as one of the more enigmatic plutonic episodes of the Proterozoic North American craton. The amount of crustal readjustment during its 80-Ma history of formation is certainly profound. If the southwestern United States is typical, 15 to 40 percent of the exposed upper Proterozoic crust formed at this time. The main form of strain affecting the upper crust during this period was simply that due to accommodation to the rise of these batholith-sized magma bodies.

Anorogenic or Simply Epizonal

Anorogenic implies the lack of any relation to orogeny. The term has all of the failings of any genetic classification and should be used in caution where knowledge of the complete deformation history of the crust is precluded by lack of exposure depth. Even in orogenic settings, the drier magmas will have the capacity to rise far from any disturbed regions and, depending on the nature of magma generation and source, may have the standard compositional and physical attributes of anorogenic magmatism. This Proterozoic case has a continent-wide expression with significant variations in exposed crustal levels. Thus, the characterization as anorogenic seems valid, as nowhere in the transcontinental province has Proterozoic orogenic deformation and metamorphism younger than 1.65 Ga been recognized. The exotic San Gabriel terrane (Silver, 1982) of southwestern California reportedly contains granulite gneisses of 1.4-Ga age, but whether this thermal event is orogenic in origin or represents heating in response to an anorogenic episode (assuming that the terrane has ties to the North American Proterozoic craton) has not been documented.

A Crustal Overturn Model

There is considerable debate regarding the origin of the anorogenic transcontinental belt, and recent models include (1) mantle diapirism in an extensional regime (J. L. Anderson and Cullers, 1978; Emslie, 1978), (2) heating in response to tectonic crustal thickening by the preceding orogenic episodes (Bickford and others, 1981; Van Schmus and Bickford, 1981), and (3) an early inland manifestation of the Grenville Orogeny (Nelson and DePaolo, 1985).

Each of these models has some obvious failings. With regard to model 1, no tectonic expression of 1.4- to 1.5-Ga extension has been recognized within the continent. For model 2, it should be noted that the transcontinental anorogenic belt cuts across all three of the orogenic provinces designated in figure 1 and did not begin to form until orogenic activity had ceased for 170 to 350 Ma. Model 3 is based on a Nd-Sm analysis of a Llano (Texas) batholith with a 1.1-b.y. crystallization and a 1.35-b.y. crust-formation age. Although the latter may indicate that the crustal source for the Llano granite separated from the mantle 1.35 Ga ago, it could also represent a mixture of source age, including Grenvillian and something much older, such as 1.7 to 1. 9 b.y.

The most serious failing of all of these models is a presumption of a Phanerozoic tectonic analogue. There is no doubt that the Proterozoic has many similarities to the Phanerozoic, yet there are major differences—the episodic nature of the Proterozoic orogenies on a worldwide basis (Condie, 1982, p. 96-97) and the high rate of continental growth during these orogenic periods of crust formation. Figure 1 depicts the relative proportions of Archean and Proterozoic crust of North American craton. The early Proterozoic orogenies (1.95 to 1.65 Ga) created an enormous amount of new continental crust. The preceding and succeeding periods, 2.6 to 1.95 Ga and 1.65 to 1.1 Ga, respectively, were a time of worldwide tectonic quiescence for which there is no Phanerozoic anologue. The cause of this quiescence is uncertain. One implication is that the rate of plate consumption dramatically slowed. A more reasonable explanation is that plate consumption became intraoceanic, which is probable if Piper's (1985) model for a Proterozoic supercontinent remains valid.

The model presented here assumes that this new crust was vertically undifferentiated (i.e., no Conrad Discontinuity) with a potential low-melting fraction that would be susceptible to partial fusion and melt segregation pending arrival of a thermal perturbation. This new crust also rested on a mantle that, now isolated from suboceanic processes, would be less depleted of its own low-melting fraction, as is the case for some portions of the modern-day subcontinental mantle (DePaolo and Wasserburg, 1976). Eventual heating and diapiric rise of a destabilized but solid mantle plume could lead, depending on the P-T path, to the formation of large gabbroic magma chambers that would, in absence of continental rifting, underplate or intrude the lower crust. Building on the model of Barker and others (1975), the resultant thermal upwelling, with or without mantle melting, would induce a profound disturbance in the lower crust leading to formation and separation of potassic granitic magma. This process would continue until both the mantle and relatively young Proterozoic crust reached a stable configuration. The eventual result is that the mantle would be free of its deeper, thermally unstable component and the crust would be differentiated into lower mafic crust of residual composition and an upper felsic crust derived from intrusion and extrusion of these granitic magmas. The model explains several features of the Proterozoic anorogenic event: (1) the association but not ubiquitous occurrence of anorthosite with the granites of this age; (2) many Proterozoic anorthosites and diabase dikes have only mildly depleted to near chondritic ϵ_{Nd} values (DePaolo and Wasserburg, 1976; Ashwal and others, 1985); (3) the entire province is contained within older Proterozoic orogenic crust; and (4) this staggering amount of anorogenic upper crustal intrusion on a continent-wide basis has no Phanerozoic equivalent.

SUMMARY

Representing a portion of the 1.4- to 1.5-Ga transcontinental belt, numerous anorogenic potassic granites occur in the Proterozoic exposures of Arizona, southern Nevada, and southeastern California, all having ages between 1.40 and 1.45 Ga. Their mineralogy and petrologic nature lead to the following conclusions.

(1) As implied for their usual K-feldspar megacrystic character, the granites are more potassic, have higher Fe-Fe+Mg ratios, and are lower in Mg, Ca, Na, and Sr than most of the older, orogenic granitoids that form parts of the host terranes.
(2) All belong to an anorogenic magnetite series, but significant variations exist in their hydrous and accessory mineralogy. A peraluminous biotite to two-mica suite, which generally contains monazite but lacks fluorite, resides in central to southeastern Arizona. A metaluminous to marginally peraluminous suite of biotite + sphene ± hornblende ± fluorite occurs from southern Arizona to California and north along the Colorado River to southern Nevada. The boundary between these two contrasting granitic suites, at least on its western extent, coincides with a major change in the preceding metamorphic and magmatic history of the host terrane.
(3) The above regional variation must reflect compositional and mineralogical changes of a lower crustal source (≥25 to 37 km). The preferred composition is a calc-alkaline metaigneous source with significant contribution of a metasedimentary component for the more peraluminous segment. Recent Nd-Sm studies show the source to be Proterozoic in age with a residence period ranging from 250 to 400 Ma.
(4) The potassic and LILE-enriched composition of the granites is a result of limited melting due to a lower water content of the source. However, this enrichment is less elevated for granites hosted in the more youthful orogenic terrane of southeastern Arizona, a probable consequence of greater melting of a source that was less dry and had a larger metasedimentary component.
(5) Due to low water fugacities (lower for the metaluminous granites), the plutons intruded into the upper crust at depths of 8 to 17 km or shallower. Feldspar thermometry yields an estimated temperature range of 620-790°C.
(6) Directly indicative of regional variations of the oxidized state of the source, the granites crystallized at elevated oxygen fugacities spanning three orders of magnitude. The most elevated oxygen levels were recorded for the Hualapai Mountains, where biotite Fe/Fe+Mg drops to a low of 0.27, down from typical levels of 0.54 to 0.75.

This anorogenic magmatism of the southwest is representative not only of a transcontinental but a global event unique to the Middle Proterozoic era. It followed an equally unique Early Proterozoic time of unusually rapid crust formation and perhaps assembly of a supercontinent. A probable scenario is that the juvenile crust, largely undifferentiated, was susceptible to partial melting in response to heating and rise of thermal plumes originating in the undepleted and heating subcontinental mantle. The ensuing turnover led to considerable transfer of material from the lower to the upper crust in a process not unlike that occurring in the underlying mantle. The eventual result was lithospheric stabilization.

ACKNOWLEDGMENTS

The author wishes to acknowledge Stephen J. Reynolds who directed the author to exposures of many of the Proterozoic granites of central and southeastern Arizona. In addition, the author has gained immeasurably from the work of four of his graduate students, who sought to unravel the petrologic complexities of the Proterozoic, namely Jim Podruski, Valerie Krass, Kweepin Kwok, and Sue Orrell. Stan Keith and Chuck Thorman generously provided unpublished rock chemistry that added greatly to the data base utilized in this study. Critical reviews of this manuscript, or discussions therein, were provided by Phil Anderson, Warren Day, Stan Keith, Steve Reynolds, and Chuck Thorman. This work was in part funded by the Rudolf C. Foss Endowment for Mineralogic Research and NSF grants EAR-8417017 (with G. A. Davis) and EAR-8120880. Many of the new rock analyses utilized in this project were completed by Ray Skelly, and Patty White did a number of modal determinations of central and southeastern Arizona rock specimens. Finally, the masterful efforts of Sue Turnbow, who skillfully typed this manuscript into its final form, are sincerely appreciated.

REFERENCES

Anderson, C. A., and Creasey, S. G., 1958, Geology and ore deposits of the Jerome area, Yavapai County, Arizona: U.S. Geological Survey Professional Paper 308, 185 p.

Anderson, C. A., Scholz, E. A., and Strobell, J. D., Jr., 1955, Geology and ore deposits of the Bagdad area, Yavapai County, Arizona: U.S. Geological Survey Professional Paper 278, 103 p.

Anderson, C. A., Blacet, P. M., Silver, L. T., and Stern, T. W., 1971, Revision of the Precambrian stratigraphy in the Prescott-Jerome area, Yavapai County, Arizona: U.S. Geological Survey Bulletin 1324-C, p. C1-C16.

Anderson, J. L., 1980, Mineral equilibria and crystallization conditions in the late Precambrian Wolf River rapakivi massif, Wisconsin: American Journal of Science, v. 280, p. 289-332.

Anderson, J. L., 1983, Proterozoic anorogenic granite plutonism of North America, *in* Medaris, L.G., Mickelson, D.M., Byers, C.W., Shanks, W.C., eds., Proterozoic Geology: Geological Society America Memoir 161, p. 133-154.

Anderson, J. L., 1984, Mineralogy and crystallization conditions of Proterozoic anorogenic granites of the Colorado Front Range [abs.]: Geological Society of America Abstracts with Programs, v. 16, No. 4, p. 213.

Anderson, J. L., 1987, The Wolf River batholith: Geological Society of America, DNAG Volume—Precambrian: Conterminous U.S. (in press).

Anderson, J. L., and Cullers, R. L., 1978, Geochemistry and evolution of the Wolf River batholith, a late Precambrian rapakivi massif in North Wisconsin, USA: Precambrian Research, v. 7, p. 287-324.

Anderson, J. L., Davis, G. A., and Frost, E. G., 1979, Field guide to regional Miocene detachment faulting and early Tertiary(?) mylonitic terrains in the Colorado River Trough, southeastern California and western Arizona, *in* Abbott, P. L., ed., Geologic Excursions in the southern California area: San Diego State University, p. 109-133.

Anderson, J. L., and Rowley, M. C., 1981, Synkinematic intrusion of peraluminous and associated metaluminous granitic magmas, Whipple Mountains, California: Canadian Mineralogist, v. 19, p. 83-101.

Anderson, J. L., and Thomas, W. M., 1985, Proterozoic anorogenic two-mica granite plutonism: The Silver Plume and St. Vrain batholiths of Colorado: Geology, v. 13, p. 177-180.

Anderson, J. L., and Wright, J., n. d., Proterozoic history of a crystalline terrane in the Colorado River Desert region, southwestern California.

Anderson, T. H., and Silver, L. T., 1977, U-Pb isotope ages of granitic plutons near Cananea, Sonora: Economic Geology, v. 72, p. 827-836.

Ashwal, L. D., Wooden, J. L., and Emslie, R. F., 1985, Nd, Sr, and Pb isotope systematics of mid-Proterozoic dikes from the Grenville and Nain Provinces of Labrador: EOS (American Geophysical Union), v. 66, no. 18, p. 414.

Babcock, R. S., Brown, E. H., Clarke, M. D., and Livingston, D. E., 1979, Geology of the older Precambrian rocks of the Grand Canyon Part II. The Zoraster plutonic complex and related rocks: Precambrian Research, v. 8, p. 243-275.

Banks, N. G., 1980, Geology of a zone of metamorphic core complexes in southeastern Arizona, *in* Davis, G. H., Coney, P. J., and Crittenden, M., eds., Metamorphic core complexes: Geological Society of America Memoir 153, p. 177-215.

Barker, F., Wones, D. R., Sharp, W. N., and Desborough, G. A., 1975, The Pikes Peak batholith, Colorado Front Range, and a model for the origin of the gabbro-anorthosite-syenite-potassic granite suite: Precambrian Research, v. 2, p. 97-160.

Bennett, V., 1984, personal communication: Department of Earth and Space Sciences, University of California, Los Angeles.

Bennett, V., and DePaolo, D. J., 1984, The definition of crustal provinces in the southern Rocky Mountain region using Sm-Nd isotopic characteristics [abs.]: Geological Society of America Abstracts with Programs, v. 16, no. 4, p. 214.

Bickford, M. E., Van Schmus, W. R., and Zietz, I., 1981, Interpretation of Proterozoic basement in the midcontinent [abs.]: Geological Society of America Abstracts with Programs, v. 13, No. 7, p. 410.

Bryant, B., 1985, personal communication: U. S. Geological Survey, Denver, Colorado.

Chappell, B. W., 1979, Granites as images of their source rocks [abs.]: Geological Society of America Abstracts with Programs, v. 11, no. 7, p. 400.

Collins, W. J., Beams, S. D., White, A. J. R., and Chappell, B. W., 1982, Nature and origin of A-type granites with particular reference to southeastern Australia: Contributions to Mineralogy and Petrology, v. 80, p. 189-200.

Condie, K. C., 1978, Geochemistry of Proterozoic plutons from New Mexico, U.S.A.: Chemical Geology, v. 21, p. 131-149.

Condie, K. C., 1982, Plate tectonics and crustal evolution: New York, Pergamon Press (2nd edition), 310 p.

Cooper, J. R., and Silver, L. T., 1964, Geology and ore deposits of the Dragoon quadrangle, Cochise County, Arizona: U.S. Geological Survey Professional Paper 416, 196 p.

Couch, N. P., 1981, Metamorphism and reconnaissance geology of the eastern McDowell Mountains, Maricopa County, Arizona: Tempe, Arizona State University, unpublished M. S. thesis, 57 p.

Creasey, S. C., 1965, Geology of the San Manual area, Pinal County, Arizona: U.S. Geological Survey Professional Paper 471, 64 p.

Cullers, R. L., Koch, R., and Bickford, M. E., 1981, Chemical evolution of magmas in the igneous terrane of the St. Francois Mountains, Mo., Part II, trace element evidence: Journal of Geophysical Research, v. 86, p. 10388-10401.

Davis, G. A., Anderson, J. L., Frost, E. G., and Shackelford, T. J., 1980, Mylonitization and detachment faulting in the Whipple-Buckskin-Rawhide Mountains terrane, southeastern California and western Arizona, *in* Davis, G. H., Coney, P. J., and Crittenden, M., eds., Metamorphic core complexes: Geological Society of America Memoir 153, p. 79-129.

Davis, G. A., Anderson, J. L., Martin, D. L., Krummenacher, D., Frost, E. G., and Armstrong, R. L., 1982, Geologic and geochronologic relations in the lower plate of the Whipple Detachment fault, Whipple Mountains, southeastern California: a progress report, *in* Frost, E., and Martin, D. L., eds. Mesozoic-Cenozoic tectonic evolution of the Colorado River region, California, Arizona, and Nevada: San Diego, California, Cordilleran Publishers, p. 409-432.

De Paolo, D. J., and Wasserburg, G. J., 1976, Inferences about magma sources and mantle structure from variations of $^{143}Nd/^{144}Nd$: Geophysical Research Letters, v. 3, no. 12, p. 743-746.

Dexter, J. J., Goodknight, C. S., Dayvault, R. D., and Dickson, R. E., 1983, Mineral evaluation of part of the Gold Butte district, Clark Co., Nevada: Department of Energy Open File Report GJBX-18, 31 p.

Drewes, Harald, 1968, New and revised stratigraphic names in the Santa Rita Mountains of southeastern Arizona: U.S. Geological Survey Bulletin 1274-C, p. 1-15.

Drewes, Harald, 1976, Plutonic rocks of the Santa Rita mountains, southeast of Tucson, Arizona: U.S. Geological Survey Professional Paper 915, 76 p.

Emslie, R. F., 1978, Anorthosite massifs, rapakivi granites, and late Proterozoic rifting of North America: Precambrian Research, v. 7, p. 61-98.

Farmer, G. L., and DePaolo, D. J., 1984, Origin of Mesozoic and Tertiary granite in the western United States and implications for Pre-Mesozoic crustal structure 2. Nd and Sr isotopic studies of mineralized and Cu- and Mo-mineralized granite in the Precambrian craton: Journal of Geophyical Research v. 89, no. B12, p. 10141-10160.

Grubensky, M., 1984, personal communication: U.S. Geological Survey, Menlo Park, California.

Hammerstrom, J. M., and Zen, E-an, 1985, An empirical equation for igneous calcic amphibole geobarometry [abs.]: Geological Society of America Abstracts with Programs, v. 17, no. 7, p. 602.

Hayes, P. T., and Raup, R. B., 1968, Geologic map of the Huachuca and Mustang Mountains, southeastern Arizona: U.S. Geological Survey Miscellaneous Geological Investigation Map I-509.

Hazelton, H. T., Hovis, G. L., Hemingway, B. S., and Robie, R. A., 1982, Calorimetric investigation of the excess entropy of mixing in analbite-sanidine solid solutions: lack of evidence for Na, K short range order and implications for two-feldspar thermometry: American Mineralogist, v. 68, p. 398-413.

Irvine, T. N., and Baragar, W. R. A., 1971, A guide to the chemical composition of the common volcanic rocks: Canadian Journal of Earth Sciences, v. 8, p. 523-548.

Ishihara, S., 1977, The magnetite-series and ilmenite-series granitic rocks: Mining Geology, v. 27, p. 293-305.

Keith, S. B., 1984, personal communication: Geologist, Magmachem Inc., Phoenix, Arizona.

Keith, S. B., Reynolds, S. J., Damon, P. E., Shafiqullah, M., Livingston, D. E., and Pushkar, P. D., 1980, Evidence for multiple intrusion and

deformation within the Santa Catalina-Rincon-Tortolita crystalline complex, southeastern Arizona, *in* Davis, G. H., Coney, P. J., and Crittenden, M., eds., Metamorphic core complexes: Geological Society of America Memoir 153, p. 217-267.

Kessler, E. J., 1976, Rb-Sr geochronology and trace element geochemistry of Precambrian rocks in the northern Hualapai Mountains, Mojave County, Arizona: Tucson, University of Arizona, unpublished M. S. thesis, 73 p.

Krass, V. A., 1980, Petrology of upper plate and lower plate crystalline terranes, Bowman's Wash area of the Whipple Mountains, southeastern California: Los Angeles, University of Southern California, unpublished M. S. thesis, 252 p.

Krieger, M.H., 1965, Geology of the Prescott and Paulden quadrangles, Arizona: U.S. Geological Survey Professional Paper 467, 127 p.

Kwok, K., 1983, Petrochemistry and mineralogy of anorogenic granites of the southwestern United States: Los Angeles, University of Southern California, unpublished M.S. thesis, 149 p.

Kwok, K. and Anderson, J.L., 1983, Proterozoic anorogenic granites of the southwestern U.S.: petrochemistry and mineralogy [abs.]: Geological Society of American Abstracts with Programs, V. 15, No. 5, p. 412.

Leake, B. E., 1978, Nomenclature of amphiboles: Canadian Mineralogist, v. 16, p. 501-520.

Lindsley, D. H., 1976, Experimental studies of oxide minerals, in Rumble, D., ed., Oxide minerals: Mineralogical Society of America Short Course Notes, v. 3, p. L61-L84.

Livingston, D. E., 1969, Geochronology of older Precambrian rocks in Gila County, Arizona: Tucson, University of Arizona, unpublished Ph.D. dissertation, 224 p.

Loiselle, M. C., and Wones, D. R., 1979, Characteristics and origin of anorogenic granites [abs]: Geological Society of American Abstracts with Programs. v. 11, no. 7, p. 468.

Miller, C. F., Stoddard, E. F., Bradfish, L. J., and Dollase, W. A., 1981, Composition of plutonic muscovite: genetic implications: Canadian Mineralogist, v. 19, p. 25-34.

Nelson, B. K., and DePaolo, D. J., 1985, Rapid production of continental crust 1.7-1.9 b.y. ago: Nd and Sr isotopic evidence from the basement of the North American midcontinent: Geological Society of America Bulletin, v. 96, p. 746-754.

Peterson, N. P., 1938, Geology and ore deposits of the Mammoth Mining camp area, Pinal Co., Arizona: Tucson, University of Arizona, Arizona Bureau Mines, Bulletin 144, 63 p.

Piper, J. D., 1983, Dynamics of the continental crust in Proterozoic times, *in* Medaris, L. G., Mickelson, D. M., Byers, C. W., and Shanks, W. C., eds., Proterozoic geology: Geological Society of America Memoir 161, p. 11-34.

Podruski, J. A., 1979, Petrology of the upper plate crystalline complex in the eastern Whipple Mountains, San Bernardino County, California: Los Angeles, University of Southern California, unpublished M.S. thesis, 193 p.

Pushkar, P. G., and Damon, P. E., 1974, Apparent Paleozoic ages from southern Arizona: K-Ar and Rb-Sr geochronology: Isochron/West, No. 10, p. 7-10.

Ransome, F. L., 1903, Geology of the Globe Copper district, Arizona: U.S. Geological Survey Professional Paper 12, 168 p.

Sauck, W. A., and Sumner, J. S., 1970, Residual aeromagnetic map of Arizona: Tucson, University of Arizona, Department of Geosciences, scale 1:1,000,000.

Schwartz, G. M., 1953, Geology of the San Manuel copper district, Arizona: U.S. Geological Survey Professional Paper 256, 63 p.

Shakel, D. W., Silver, L. T., and Damon, P. E., 1977, Observations on the history of the gneissic core complex, Santa Catalina Mountains, southern Arizona [abs.]: Geological Society of America Abstracts with Programs, v. 9, p. 1169-1170.

Silver, L. T., 1968, Precambrian batholiths of Arizona: Geological Society of America Special Paper 121, p. 558-559.

Silver, L. T., 1978, Precambrian formations and Precambrian history in Cochise County, southeastern Arizona, *in* Callender, J. F., Wilt, J. C., and Clemons, R. E., eds., Land of Cochise: Socorro, New Mexico Geological Society, 29th Field Conference Guidebook, p. 157-163.

Silver, L. T., 1982, Evolution of crystalline rock terranes of the Transverse Ranges, southern California [abs.]: Geological Society of America Abstracts with Programs, v. 14, p. 234.

Silver, L. T., Bickford, M. E., Van Schmus, W. R., Anderson, J. L., Anderson, T. H., and Medaris, L. G., Jr., 1977, The 1.4-1.5 b.y. transcontinental anorogenic plutonic perforation of North America [abs.]: Geological Society of America Abstracts with Programs, v. 9, no. 7, p. 1176-1177.

Silver, L. T., and McKinney, C. R., 1962, U-Pb isotope age studies of a Precambrian granite, Marble Mountains, San Bernardino County, California: Geological Society of America Special Paper 73, p. 65.

Silver, L. T., Williams, I. S., and Woodhead, J. A., 1981, Uranium in granites from the southwestern United States: actinide parent-daughter system, sites, and mobilization: U.S. Department of Energy Open File Report GJBX-45, 315 p.

Sommer, J. V., 1982, Structural geology and metamorphic petrology of the northern Sierra Estrella, Maricopa County, Arizona: Tempe, Arizona State University, unpublished M. S. thesis, 127 p.

Stewart, J. H., and Carlson, J. E., 1978, Geologic map of Nevada, scale 1:500,000.

Swan, M. M., 1976, The Stockton Pass fault: An element of the Texas lineament: Tucson, University of Arizona, unpublished M. S. thesis, 119 p.

Thomas, W. M., Clarke, H. S., Young, E. D., Orrell, S. E., and Anderson, J. L., in press, Precambrian granulite facies metamorphism in the Colorado River region, Nevada, Arizona, and California, *in* Ernst, W. G., ed., Metamorphic and crustal evolution of the western conterminous U.S.—Rubey Volume VII: Englewood Cliffs, New Jersey, Prentice-Hall.

Thorman, C. H., 1982, Geology of the Pinaleno Mountains, Arizona: a preliminary report, *in* Stone, Claudia, and Jenney, J. P., eds.: Arizona Geological Society Digest, v. 13, p. 5-12.

Thorman, C. H., 1984, written communication: U.S. Geological Survey, Denver, Colorado.

Thorpe, D., 1980, Mineralogy and petrology of Precambrian metavolcanic rocks, Squaw Peak, Phoenix, Arizona: Tempe, Arizona State University, unpublished M. S. thesis, 115 p.

Van Schmus, W. R., and Bickford, M. E., 1981, Proterozoic chronology and evolution of the midcontinent region, North America, *in* Kroner, A., ed., Precambrian plate tectonics: New York, Elsevier Science Publishers, p. 261-296.

Volborth, A., 1962, Rapakivi-type granites in the Precambrian complex of Gold Butte, Clark County, Nevada: Geological Society of America Bulletin, v. 73, p. 813-832.

Volborth, A., 1973, Geology of the granite complex of the Eldorado, Newberry, and northern Dead Mountains, Clark County, Nevada: Nevada Bureau of Mines and Geology Bulletin, v. 80, 40 p.

Vorma, A., 1971, Alkali feldspars of the Wiborg rapakivi massif in southeastern Finland: Bulletin de la Commission Geologique de la Finlande, v. 246, p. 1-72.

Wones, D. R., 1979, Intensive parameters during crystallization of granitic plutons: Geological Society of America Abstracts with Programs, v. 11, p. 543.

Wones, D. R., 1981, Mafic silicates as indicators of intensive variables in granitic magmas: Mining Geology, v. 31, p. 191-212.

Wright, J., 1984, personal communication: Department of Geology, Stanford University.

Young, E. D., 1985, personal communication: Department of Geological Sciences, University of Southern California.

Revised manuscript accepted 1987.

APPENDIX 1. Major-element, Trace-element and Modal Analyses

	Gold Butte						Beer Bottle			Newberry		Davis Dam	
	GB-3	GB-6	516	537	564	646	841A	841D	844B	NY6a	NY6b	NY13A	NY11A
SiO_2	66.06	66.76	67.58	68.10	70.60	74.05	65.99	67.77	66.68	65.20	64.03	66.49	70.36
TiO_2	0.68	0.53	0.89	0.83	0.95	0.60	0.97	0.98	1.12	1.24	1.35	0.85	0.65
Al_2O_3	15.59	15.31	13.64	13.80	13.79	13.08	14.49	14.45	14.13	13.62	14.34	14.38	13.40
FeO[1]	3.17	6.23	3.54	3.28	3.63	2.76	5.03	4.30	5.28	5.67	6.38	4.92	4.81
MgO	0.81	0.43	0.70	0.66	0.71	0.53	0.66	0.55	0.79	1.41	1.53	1.04	0.78
MnO	0.068	0.059	0.080	0.080	0.080	0.060	0.105	0.090	0.100	0.077	0.130	0.120	0.063
CaO	1.99	1.43	2.27	1.97	2.10	1.75	2.81	2.52	2.91	3.17	3.75	2.28	1.90
Na_2O	3.12	2.86	2.92	2.90	2.97	2.88	2.68	2.78	2.62	2.80	2.74	3.08	2.45
K_2O	6.69	7.15	4.56	4.92	4.79	4.98	4.97	5.01	4.52	3.75	3.97	4.65	5.31
LOI	1.08	1.28	0.45	0.35	0.51	.036	-	-		1.41	0.92	0.67	0.75
TOTAL	99.26	102.04	96.84	97.10	100.13	101.05	97.74	98.44	98.15	98.35	99.14	98.48	100.48
FeO/FeO+MgO	.796	.935	.835	.832	.836	.839	.844	.887	.870	.801	.807	.826	.860
A/CNK[2]	.975	1.018	.984	1.009	.993	.983	.973	.993	.975	.944	.918	1.010	1.013
Rb[3]	258	294	-	-	-	-	182	200	192	182	156	263	225
Sr	250	226	-	-	-	-	325	312	309	274	281	155	176
Ba	2465	2148	1600	1450	1450	1500	1353	1287	1305	1033	1091	770	857
Quartz	20.5	23.9					22.6	18.4		22.8	17.5	23.1	26.0
K-feldspar	38.8	31.8		N			32.4	31.0		21.1	24.8	32.8	31.0
Plagioclase	21.5	26.1		o			25.0	28.8		34.2	33.1	24.0	27.0
Biotite	7.5	9.9					10.5	16.4		9.9	14.6	15.2	11.6
Hornblende		0.2		M			4.7	0.3		3.2	5.1	-	-
Sphene	3.4	2.2		o			1.1	1.3		1.5	0.3	1.5	0.2
Muscovite	-	-		d			-	-		-	-	-	-
Allanite	0.9	0.6		a			<0.1	0.1		2.5	0.2	0.6	0.2
Apatite	0.9	0.6		l			0.8	0.5		0.5	0.4	0.1	0.3
Zircon	1.4	0.8					0.1	0.1		<0.1	<0.1	0.7	0.2
Monazite	-	-		D			-	-		-	-	-	-
Opaques	1.6	0.5		a			2.1	1.6		1.3	1.2	1.9	2.0
Fluorite	0.6	-		t			-	-		-	-	-	-
Chlorite	0.2	-		a			<0.1	0.1		-	-	-	0.4
Sericite	2.5	3.0					0.3	0.6		2.9	2.1	-	1.1
Epidote	1.4	-					0.4	0.8		0.1	0.1	-	-
TOTAL	100.0	100.0					100.0	100.00		100.00	100.0	100.0	100.0
Ref.[4]	14	14	13	13	13	13	33	33	33	14	14	14	14

APPENDIX 1. Major-element, Trace-element and Modal Analyses (continued)

	Dead	Homer	Marble					Holy Moses				Hualapai			
	DM1C	HM-4	MB2A	MB1B	MB1A	MB2B	MB5B	HP1A2	HP1B1	HP1B2	HPD-2	HP7	HP3	HP2	HPD-8
SiO_2	73.71	70.53	67.84	68.35	69.56	68.67	69.50	67.05	67.90	68.28	69.7	66.67	68.44	71.00	73.10
TiO_2	0.19	0.40	0.67	0.61	0.60	0.66	0.50	0.98	0.86	0.84	0.50	0.39	0.49	0.35	0.60
Al_2O_3	13.87	14.45	13.02	13.48	13.73	13.60	14.25	13.39	12.65	12.91	13.80	15.00	14.65	13.27	13.37
FeO[1]	0.90	2.18	4.27	3.97	4.03	4.24	3.60	7.01	5.91	5.91	4.88	2.40	2.67	2.41	2.03
MgO	0.16	0.49	0.79	0.73	0.72	0.77	0.54	0.83	0.56	0.60	0.22	0.58	0.57	0.31	0.26
MnO	0.036	0.027	0.067	0.059	0.065	0.062	0.058	0.070	0.081	0.075	0.08	0.039	0.051	0.030	0.03
CaO	0.69	1.29	1.96	2.26	1.98	1.90	1.50	2.94	2.43	2.59	2.75	1.05	1.56	1.12	1.05
Na_2O	3.83	2.81	2.43	2.37	2.58	2.46	3.50	2.95	2.48	2.62	2.85	3.74	3.43	3.52	3.02
K_2O	5.44	6.29	4.96	5.72	5.32	5.04	5.69	3.82	4.93	4.73	4.92	7.84	6.54	5.81	6.29
LOI	0.58	0.61	1.29	1.27	1.36	1.31	1.38	0.36	0.57	0.73	-	0.72	0.62	0.95	-
TOTAL	99.41	99.08	97.30	98.82	99.95	98.71	100.52	99.40	98.37	99.29	99.70	98.43	99.02	98.77	99.75
FeO/FeO+MgO	.850	0.816	.844	.845	.848	.846	.870	.894	.913	.908	.957	.805	.824	.886	.887
A/CNK[2]	1.032	1.049	1.007	.950	1.010	1.050	.973	.934	.915	.913	.919	.907	.942	.940	.997
Rb[3]	89.9	163	423	438	391	407	449	143	197	210	226	181	192	286	195
Sr	79.8	209	119	127	124	120	136	173	113	111	120	732	806	388	606
Ba	334	893	632	725	739	603	692	1200	979	936	-	1520	1706	675	-
Quartz	30.3	25.4	19.7	17.0	22.0	24.6	32.4	15.3	11.5	10.6	N	20.3	19.6	24.4	N
K-feldspar	49.4	34.8	48.4	47.0	36.3	42.1	37.1	45.8	48.6	52.5	o	58.6	51.7	55.9	o
Plagioclase	18.4	34.9	20.7	26.0	24.2	24.0	25.1	33.5	27.7	23.9		16.2	17.0	14.2	
Biotite	0.2	3.4	6.7	6.1	8.8	5.6	2.8	2.0	4.0	2.4	M	1.5	2.7	0.6	M
Hornblende	-	-	-	-	-	-	-	0.7	4.2	2.5	o	1.3	0.9	0.5	o
Sphene	0.6	0.2	-	-	-	0.1	0.7	1.2	1.3	<0.1	d	<0.1	3.9	0.3	d
Muscovite	-	-	-	-	-	-	-	-	-	-	a	-	-	-	a
Allanite	-	<0.1	1.1	0.8	0.6	0.7	<0.1	<0.1	0.5	<0.1	l	0.2	<0.1	<0.1	l
Apatite	<0.1	0.1	0.7	0.2	0.4	0.3	<0.1	0.2	0.7	1.9		0.1	<0.1	0.7	
Zircon	<0.1	<0.1	0.4	0.7	0.9	0.8	0.2	<0.1	0.9	1.5	D	0.1	<0.1	<0.1	D
Monazite	-	-	-	-	-	-	-	-	-	-	a	-	-	-	a
Opaques	0.2	0.8	0.8	0.5	0.5	0.5	0.2	1.4	0.2	4.7	t	0.8	1.6	1.6	t
Fluorite	-	-	0.3	0.1	0.1	-	-	-	0.2	-	a	<0.1	<0.1	0.5	a
Chlorite	0.1	0.2	0.4	0.4	1.2	0.8	0.3	-	-	-		-	-	0.2	
Sericite	0.7	0.1	0.6	1.0	4.4	0.4	0.8	-	0.2	-		0.1	-	0.1	
Epidote	-	0.1	0.4	0.2	0.5	0.1	0.1	-	-	-		0.7	2.6	-	
TOTAL	100.0	100.0	100.1	100.0	100.0	100.0	100.1	100.1	100.00	100.0		100.0	100.0	100.0	
Ref.[4]	14	14	14	14	14	14	14	14	14	14	3	14	14	14	3

APPENDIX I. Major-element, Trace-element and Modal Analyses (continued)

	Bowmans Wash									Parker Dam									
	VM95	JP44	VM96	W7818	JP410	VA52	L113	JP413	JP200	7828	7831	7825a	7835	JP280	JP281	7826	78430	JP282	JP412
SiO_2	60.69	60.85	61.05	61.28	61.32	63.46	63.47	63.65	63.75	64.67	65.03	66.20	66.24	66.33	67.42	67.83	68.11	69.41	69.88
TiO_2	1.81	1.47	1.84	1.49	1.36	1.30	1.32	1.30	1.35	1.21	1.39	0.96	1.00	0.99	0.74	0.88	0.50	0.38	0.59
Al_2O_3	13.87	13.64	13.41	13.67	13.76	13.87	13.95	13.17	13.43	12.91	13.29	14.46	14.13	13.29	14.65	14.13	14.53	15.03	13.55
FeO[1]	8.79	8.71	8.80	8.28	8.07	6.61	6.92	7.74	7.85	7.21	6.86	5.34	5.83	5.51	4.42	4.62	3.20	2.49	4.06
MgO	1.88	1.62	1.87	1.65	1.58	1.34	1.39	1.38	1.53	1.40	1.36	1.18	1.11	1.06	0.86	0.96	0.55	0.46	0.63
MnO	0.15	0.147	0.140	0.128	0.120	0.110	0.100	0.132	0.130	0.122	0.108	0.076	0.096	0.093	0.072	0.061	0.042	0.038	0.053
CaO	4.48	4.42	4.26	4.09	4.15	3.24	3.35	3.88	3.81	2.87	3.38	2.86	2.95	2.79	1.54	2.38	1.41	1.56	1.67
Na_2O	2.70	2.59	2.70	3.05	2.81	2.94	2.83	2.64	2.66	2.74	2.77	2.85	2.84	2.75	2.55	2.94	2.31	2.75	2.38
K_2O	3.82	4.05	3.77	3.96	4.03	4.81	4.59	4.30	4.30	4.26	4.35	5.06	4.63	4.96	6.58	4.94	7.04	6.61	6.14
LOI	1.07	nd	1.14	1.46	nd	1.14	1.02	nd	nd	0.87	1.17	1.72	.87	nd	nd	nd	nd	-	nd
TOTAL	99.06	97.50	98.98	99.08	97.20	98.92	98.94	98.19	98.81	98.26	99.71	100.69	99.69	97.77	98.83	99.63	97.69	98.73	97.86
FeO/FeO+MgO	0.823	.843	.825	.833	.836	.831	.833	.849	.837	.837	.835	.819	.840	.839	.837	.829	.853	.844	.866
A/CNK[2]	.818	.818	.825	.817	.833	.861	.888	.821	.842	.901	.863	.941	.939	.888	1.038	.974	1.039	1.036	.997
Rb[3]	116	106	133	115	125	204	190	138	119	164	170	173	195	220	309	186	263	358	292
Sr	304	278	275	325	284	212	222	284	284	109	216	207	190	194	163	182	159	152	183
Ba	1334	1644	1219	1296	1487	1381	1301	1357	1507	1107	1101	1235	986	957	1181	1035	-	1087	1308
Quartz	20.0	12.5	18.1	24.3	14.9	14.7	17.3	15.9	24.1	23.8	20.0	27.3	18.1	25.2	17.4	22.4	24.9	22.4	26.3
K-feldspar	13.0	21.5	18.0	17.5	17.2	22.7	15.4	17.9	14.3	27.6	33.5	34.0	35.1	42.4	54.6	40.6	44.7	49.6	58.0
Plagioclase	42.7	40.1	35.5	16.4	34.8	35.5	41.3	32.1	33.8	23.7	23.8	27.3	28.9	26.5	23.7	23.9	23.8	21.5	9.0
Biotite	14.7	12.1	18.1	19.0	19.5	21.3	19.0	5.0	11.4	12.9	11.2	7.8	11.6	1.5	2.8	9.3	3.8	3.09	3.9
Hornblende	5.5	8.9	4.5	10.9	7.6	-	0.4	20.7	9.7	5.4	6.7	-	1.6	2.5	-	-	-	-	-
Sphene	1.8	0.5	2.3	5.0	0.3	2.0	3.1	1.0	2.0	1.4	2.2	1.5	2.0	0.4	0.4	1.9	0.3	0.4	0.3
Muscovite	-	-	-	-	-	-	-	-	-	-	-	-	-	-	-	-	-	-	-
Allanite	-	0.8	-	0.5	0.4	-	-	0.1	0.5	<0.1	0.5	0.4	0.4	0.3	0.3	<0.1	0.3	0.3	0.3
Apatite	1.2	0.7	1.1	2.6	0.5	0.5	1.4	0.6	0.7	1.7	0.5	0.7	0.6	0.2	0.2	0.1	0.2	0.3	0.2
Zircon	0.2	<0.1	<0.1	<0.1	<0.1	0.7	<0.1	<0.1	<0.1	<0.1	<0.1	<0.1	<0.1	<0.1	<0.1	<0.1	<0.1	0.3	0.2
Monazite	-	-	-	-	-	-	-	-	-	-	-	-	-	-	-	-	-	-	-
Opaques	3.0	2.9	2.5	2.6	4.8	2.7	1.2	6.8	3.5	2.2	1.4	0.5	1.0	1.0	0.6	1.3	2.0	1.2	1.8
Fluorite	-	-	-	-	-	-	-	-	-	-	-	-	-	-	-	-	-	-	-
Chlorite	0.6	-	-	-	-	-	-	-	-	1.0	0.1	-	-	-	-	-	-	-	-
Sericite	-	-	-	0.8	-	-	-	-	-	0.3	-	0.5	0.4	-	-	0.5	-	-	-
Epidote	-	-	-	0.4	-	-	-	-	-	-	-	-	0.2	-	-	-	-	0.2	-
TOTAL	100.0	100.0	100.0	100.1	100.0	100.0	100.0	100.0	100.0	100.00	100.0	100.0	100.0	100.0	100.0	100.0	100.0	100.0	100.0
Ref.[4]	19	18	19	33	18	19	19	18	18	33	33	33	33	18	18	33	33	18	18

APPENDIX 1. Major-element, Trace-element and Modal Analyses (continued)

	Lawler Pk.	Dells		Sierra Estrella	Ak-Chin		Ruin			Oracle					
	LAW-1	400	DG12	SE831	MC831	MC832	83-1A	02	83-1B	83-2	83-1	S1776	Ya1	S2076	S1876
SiO_2	75.33	75.61	76.2	70.15	73.43	74.64	70.27	71.02	71.27	67.30	67.89	68.47	70.00	72.43	74.05
TiO_2	0.22	0.03	0.04	.33	.25	.25	.39	0.43	.42	.91	.83	.87	0.34	.48	.42
Al_2O_3	12.77	13.09	13.70	14.38	13.40	13.19	14.16	13.65	13.79	14.14	14.67	13.70	15.40	13.50	13.30
FeO[1]	1.35	0.73	0.79	2.36	1.38	1.16	2.49	2.51	2.53	4.56	4.33	5.65	2.36	3.30	3.29
MgO	0.42	0.05	0.10	0.66	0.34	0.28	0.71	1.11	0.74	1.12	1.10	1.33	0.52	0.71	0.71
MnO	0.070	0.030	0.03	0.082	0.073	0.077	0.087	0.070	0.095	0.127	0.133	.100	0.040	.088	0.92
CaO	1.07	0.62	0.50	2.11	1.19	0.92	1.77	1.80	1.90	2.53	2.44	2.08	1.90	1.90	1.47
Na_2O	3.09	4.14	4.20	3.20	3.13	3.02	3.03	2.92	2.99	2.97	3.17	2.25	3.40	3.24	2.39
K_2O	4.31	4.53	4.50	4.85	5.24	5.34	5.01	4.62	4.56	4.30	4.21	3.92	4.80	3.81	4.15
LOI	0.40	0.59	0.69	nd	nd	nd	nd	1.06	nd	nd	nd	nd	0.74	nd	nd
TOTAL	99.03	99.42	100.75	98.12	98.43	98.28	97.92	99.14	98.30	98.06	98.77	98.37	99.50	99.46	99.87
FeO/FeO+MgO	.763	.936	0.899	.781	.802	.806	.778	.693	.774	.797	.803	.809	.819	.823	.823
A/CNK[2]	1.092	1.020	1.080	1.002	1.032	1.062	1.039	1.044	1.036	1.033	1.007	1.169	1.081	1.046	1.199
Rb[3]	339	194	nd	190	320	358	262	275	291	202	191	152	nd	174	206
Sr	103	11.0	nd	140	61.2	54.0	136	136	135	156	154	151	nd	197	168
Ba	280	25	nd	654	267	292	543	455	425	585	700	966	nd	879	799
Quartz	34.0	35	36	32.7	35.8	39.9	30.4	28	30.2	29.6	33.6	N	31	N	N
K-feldspar	37.5	27	28	32.8	32.9	30.2	26.4	39	22.4	23.1	24.1	o	12	o	o
Plagioclase	21.7	34	25	28.2	24.4	25.5	32.8	21	34.9	30.2	29.5		40		
Biotite	2.1	2	<1	4.5	2.5	2.4	5.5	8.2	7.5	13.5	6.8	M	14	M	M
Hornblende	-	-	-	-	-	-	-	-	-	-	-	o	1	o	o
Sphene	-	-	-	<0.1	-	-	-	-	-	-	-	d	-	d	d
Muscovite	3.7	2	9	0.2	0.6	0.6	0.7	1.2	0.7	<0.1	0.3	a	-	a	a
Allanite	-	<1	nd	0.2	<0.1	<0.1	-	<1	-	-	-	l	<1	l	l
Apatite	0.1	<1	<1	0.2	0.1	<0.1	0.7	<1	0.1	0.5	0.3		-		
Zircon	0.4	<1	<1	0.2	0.4	0.1	0.2	<1	0.3	0.3	0.2	D	-	D	D
Monazite	<0.1	-	nd	<0.1	<0.1	0.1	0.1	-	<0.1	<0.1	0.2	a	-	a	a
Opaques	0.4	0.5	<1	0.6	1.1	0.6	1.9	1.0	1.3	2.5	1.6	t	2	t	t
Fluorite	0.2	<1	nd	-	<0.1	-	-	<1	-	-	-	a	-	a	a
Chlorite	-	<1	-	-	2.2	0.6	1.0	<1	1.8	-	2.9		-		
Sericite	-	<1	-	-	-	-	-	<1	-	-	0.5		<1		
Epidote	0.3	<1	-	0.4	0.2	0.2	0.4	<1	0.8	0.7	0.1		-		
TOTAL	100.0	100.5	98	100.0	100.0	100.0	100.1	98.4	100.0	100.0	100.0		100.0		
Ref.[4]	6	6	23	83	33	33	33	6	33	33	33	34	35	34	34

APPENDIX I. Major-element, Trace-element and Modal Analyses (continued)

	Continental						Fort Huachuca	
	R83-2	R83-1	DR897	1046	1220	104	83-2	83-1
SiO_2	64.24	64.43	67.40	67.40	67.80	69.40	63.52	67.55
TiO_2	.99	1.01	0.18	1.00	0.83	0.92	1.07	.63
Al_2O_3	13.97	14.13	14.40	14.30	14.00	12.40	15.25	14.33
FeO^1	5.59	5.59	4.08	4.70	4.62	4.54	5.74	3.63
MgO	1.59	1.42	1.20	0.91	1.30	0.61	1.55	1.25
MnO	0.111	0.113	0.120	0.080	0.130	0.120	0.168	0.062
CaO	2.19	2.52	2.70	3.20	2.00	1.70	1.76	1.53
Na_2O	2.99	2.70	2.80	3.30	2.30	3.80	3.00	2.71
K_2O	4.81	5.14	4.10	2.80	5.30	4.50	5.74	5.33
LOI	nd	nd	1.56	0.87	0.47	1.54	nd	nd
TOTAL	96.48	97.05	98.54	98.66	98.75	99.53	97.84	97.02
FeO/FeO+MgO	.797	.779	.811	.838	.750	.843	.787	.744
A/CNK^2	.969	.991	1.032	989	1.064	.873	1.063	1.102
Rb^3	223	195	nd	nd	nd	nd	339	367
Sr	219	211	nd	nd	nd	nd	154	121
Ba	1387	1371	nd	nd	nd	nd	873	636
Quartz	30.3	28.7	25.1	27.8	28.2	16.4	27.5	34.6
K-feldspar	19.9	25.8	12.6	30.5	15.2	38.6	28.0	36.1
Plagioclase	34.9	33.2	41.3	26.1	35.4	26.7	26.2	21.7
Biotite	-	-	16.2	11.6	15.4	11.7	11.0	-
Hornblende	-	-	-	-	-	-	-	-
Sphene	3.1	1.9	1.4	1.1	0.1	-	0.9	<0.1
Muscovite	-	-	-	-	-	-	-	-
Allanite	-	-	-	<0.1	-	-	-	<0.1
Apatite	0.4	0.4	1.0	0.9	1.0	1.0	0.8	0.3
Zircon	<0.1	0.8	<1.0	0.1	0.4	0.2	0.2	<0.1
Monazite	-	-	-	-	-	-	-	-
Opaques	2.0	1.0	2.4	1.9	4.4	2.9	3.3	1.4
Fluorite	-	-	-	-	-	-	-	-
Chlorite	7.3	7.6	-	-	-	-	1.9	5.5
Sericite	-	-	-	-	-	-	-	-
Epidote	2.1	1.2	-	-	-	-	0.2	0.4
TOTAL	100.0	100.0	100.0	100.0	100.0	100.0	100.0	100.0
Ref.[4]	33	33	31	31	31	31	33	33

[1]All Fe as FeO
[2]A/CNK = mole ratio of $Al_2O_3/(CaO+Na_2O+K_2O)$
[3]Rb, Sr, Ba as ppm
[4]References as in table 1 except for 34 (S. Keith, written comm., 1983) and 35 (Banks, 1980)